BIOMEDICAL ENGINEERING

ENHANCED INTRACELLULAR PEPTIDE DELIVERY WITH PH-RESPONSIVE, ENDOSOMOLYTIC NANO-POLYPLEXES TO MODULATE VASCULAR SMOOTH MUSCLE CELL BEHAVIOR

BRIAN CONNOR EVANS

Thesis under the direction of Professor Craig L. Duvall

Peptide-based therapeutics have significant potential for use in a variety of clinical applications ranging from cancer therapy to promotion of cardiovascular health. However, the efficacy of these approaches is limited due to poor cellular uptake and peptide sequestration within endo-lysomal vesicles that are trafficked for exocytosis or lysosomal degradation. The drug delivery platform described herein provides a means to overcome these barriers through the use of cell-permeant, pH-responsive nano-polyplexes that significantly enhance cell internalization and facilitate endosomal escape of a cationic, therapeutic peptide. A reproducible method to synthesize electrostatically complexed nanoparticles containing a therapeutic peptide and a pH-responsive polymer has been developed and optimized to yield nano-polyplexes of approximately 100 nm in diameter. These polyplexes display pH-dependent membrane disruption ideal for endosomal escape, which was verified through microscopic analysis of cellular uptake and intracellular trafficking. The polyplexes were found to have significantly enhanced bioactivity in reducing inflammatory cytokine production in stimulated human vascular smooth muscle cells *in vitro* compared to the peptide alone ($p<0.05$). Furthermore, flow cytometric analysis revealed that these polyplexes significantly enhanced cellular uptake and intracellular half-life compared to the peptide alone ($p<0.05$). This promising platform technology provides a novel method to effectively enhance cytosolic delivery of cationic therapeutic peptides and demonstrates a potentially high-impact therapeutic approach to improving graft patency in vascular bypass grafting applications.

Approved:

Professor Craig Duvall

ENHANCED INTRACELLULAR PEPTIDE DELIVERY WITH PH-RESPONSIVE, ENDOSOMOLYTIC NANO-POLYPLEXES TO MODULATE VASCULAR SMOOTH MUSCLE CELL BEHAVIOR

By

Brian Connor Evans

Thesis

Submitted to the Faculty of the

Graduate School of Vanderbilt University

in Partial Fulfillment of the Requirements

for the Degree of

MASTER OF SCIENCE

in

Biomedical Engineering

May, 2013

Nashville, Tennessee

Approved:

Professor Craig L. Duvall

Professor Colleen M. Brophy

To my parents, Debbie and David, who have given me every opportunity in life to succeed

and my family, Nanny, Eric, Rachel, Cash, and Dax who

have supported and loved me through all that I do.

ACKNOWLEDGMENTS

First and foremost, I would like to thank Dr. Craig Duvall. Without his guidance, insight, and friendship this work would not be possible. I would also like to thank Dr. Colleen Brophy for her collaboration with our lab that made this project possible, for her oversight and guidance, and for providing the resources needed to complete this work. I would like to thank Kyle Hocking and Dr. Joyce Cheung-Flynn for their aid in designing and carrying out experiments.

Additionally, I would like to thank my fellow researchers Mukesh Gupta, Chris Nelson, Martina Miteva, Kelsey Beavers, Lucas Hofmeister, Angela Zachman, Spencer Crowder, and Shann Yu for their help with experiments, day to day labwork, and support through the past three years. I would like to give a special thanks to Samantha Sarrett for her help in performing imaging for this project. Finally, I would like to thank my undergraduate research assistants Mitchell Wiesenberger and Julia Dmowska for their help in daily labwork and completing experiments.

Confocal imaging was performed using a Zeiss LSM 710 Inverted Confocal Microscope through the use of the VUMC Cell Imaging Shared Resource, (supported by NIH Grants CA68485, DK20593, DK58404, HD15052, DK59637, and Ey008126). Dynamic light scattering and TEM were conducted through the use of the core facilities of the Vanderbilt Institute of Nanoscale Sciences and Engineering (VINSE). This work was supported by NIH grant 1R21HL110056-01, AHA scientist development grant 11SDG4890030, and the NSF graduate research fellowship program.

TABLE OF CONTENTS

Appendix

LIST OF FIGURES

CHAPTER I

INTRODUCTION

Vein Graft Failure

Cardiovascular disease (**CVD**) is the leading cause of death in the United States, with coronary heart disease responsible for more than 50% of CVD-related mortality causing 1 of every 6 deaths [1]. In terms of financial burden, the direct and indirect cost of coronary heart disease in the US were ~$200 billion in 2009, with a projected price increase of 100% between 2013 and 2030 [1] Coronary artery bypass grafting with autologous conduits remains the standard treatment for multi-vessel coronary heart disease. However, almost half of saphenous vein grafts fail within the first 18 months due to intimal hyperplasia (**IH**) [2]. One of the underlying causes of IH is activation of MAPKAP Kinase II (**MK2**) signaling in vascular smooth muscle cells (**VSMCs),** which occurs due to environmental and mechanical stresses experienced by the graft during surgical resection and transplantation[3]. MK2 activation results in vasoconstriction and pathological VSMC proliferation, migration, and excess ECM production that result in graft occlusion. These effects are primarily a result of the downstream phosphorylation of heat shock protein 27 (**HSP27**) by activated MK2, which stimulates the release of inflammatory cytokines and chemotactic agents from endogenous vascular cells [4-6] (See **Fig. 1**). A variety of small molecule inhibitors of MK2 exist, but they lack specificity and none have been approved by the FDA [7]. In contrast, Hayess and Benndorf developed a highly specific peptide antagonist of MK2 [8], and a previous study suggests that intracellular delivery of peptidic MK2 inhibitor can reduce vasoconstriction and subsequent IH in human saphenous vein [4], but the efficacy of this approach is limited due to limited cellular uptake and peptide sequestration within endo-lysosomal vesicles that are trafficked for exocytosis or lysosomal degradation[9].

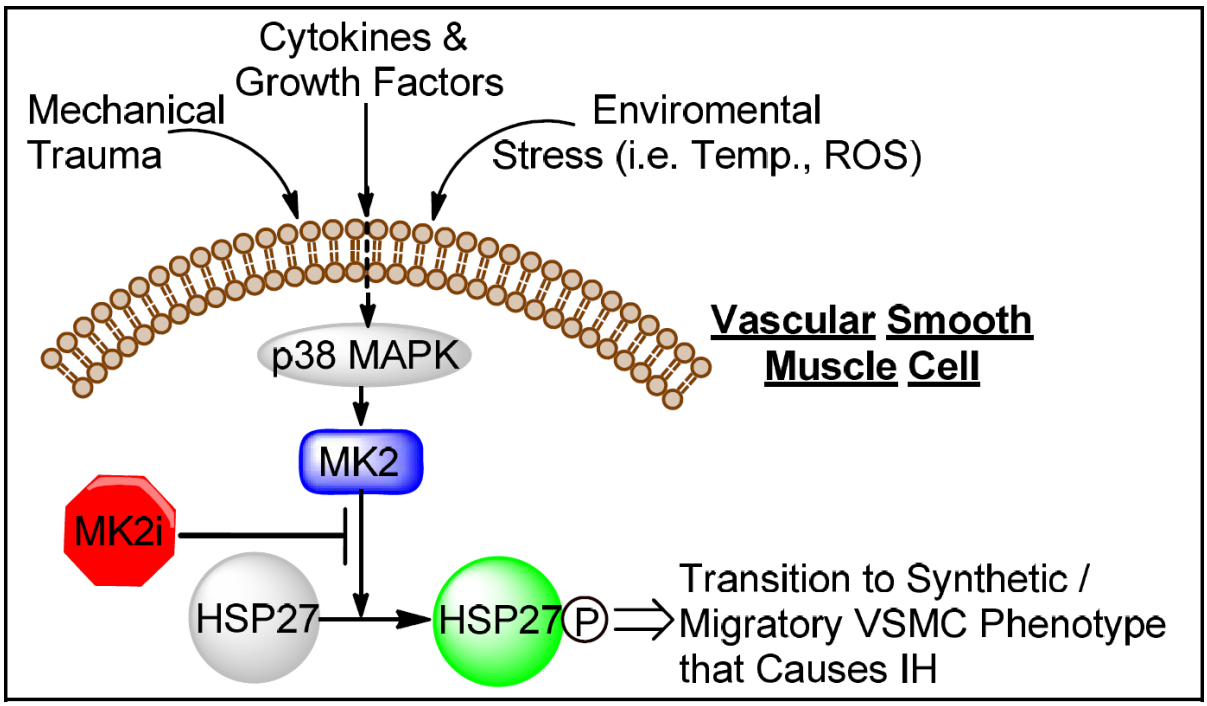

Figure 1 - P38 MAPK signaling cascade: that is activated in VSMCs during surgical resection and transplantation resulting in a pathological VSMC phenotype.

Peptide Delivery Barriers

The therapeutic potential of peptides, proteins, and antibodies in applications ranging from cancer treatments to vascular pathologies has become more apparent as the fundamental etiology of these disease states becomes more comprehensively characterized [10-16]. However, major *in vivo* barriers exist to effective intracellular delivery of peptide-based, biomacromolecular therapeutics for specific applications: proteolysis of the peptide in the *in vivo* environment prior to cellular internalization, circumvention of non-specific binding and/or side-effects, translocation across the cellular membrane, escape from the intracellular endo-lysosomal and exocytosis traffic king pathways, and achieving a therapeutically-relevant peptide dose within the intracellular micro-environment where the therapeutic target is located (see **fig. 2**) [9, 17-19]. A variety of methods have been investigated to address these delivery barriers ranging from the utilization of drug delivery vehicles that improve proteolytic resistance and in vivo half-life [20-22] to the use of electroporation, or cell-penetrant/fusogenic peptides to increase cell internalization of biomacromolecular therapeutics [23-25]. In addition to these approaches, the study and use of colloidal drug carriers such as

liposomes, micelles, and nanoparticles to deliver biomacromolecular therapeutics has increased dramatically in the past decade [26-28].

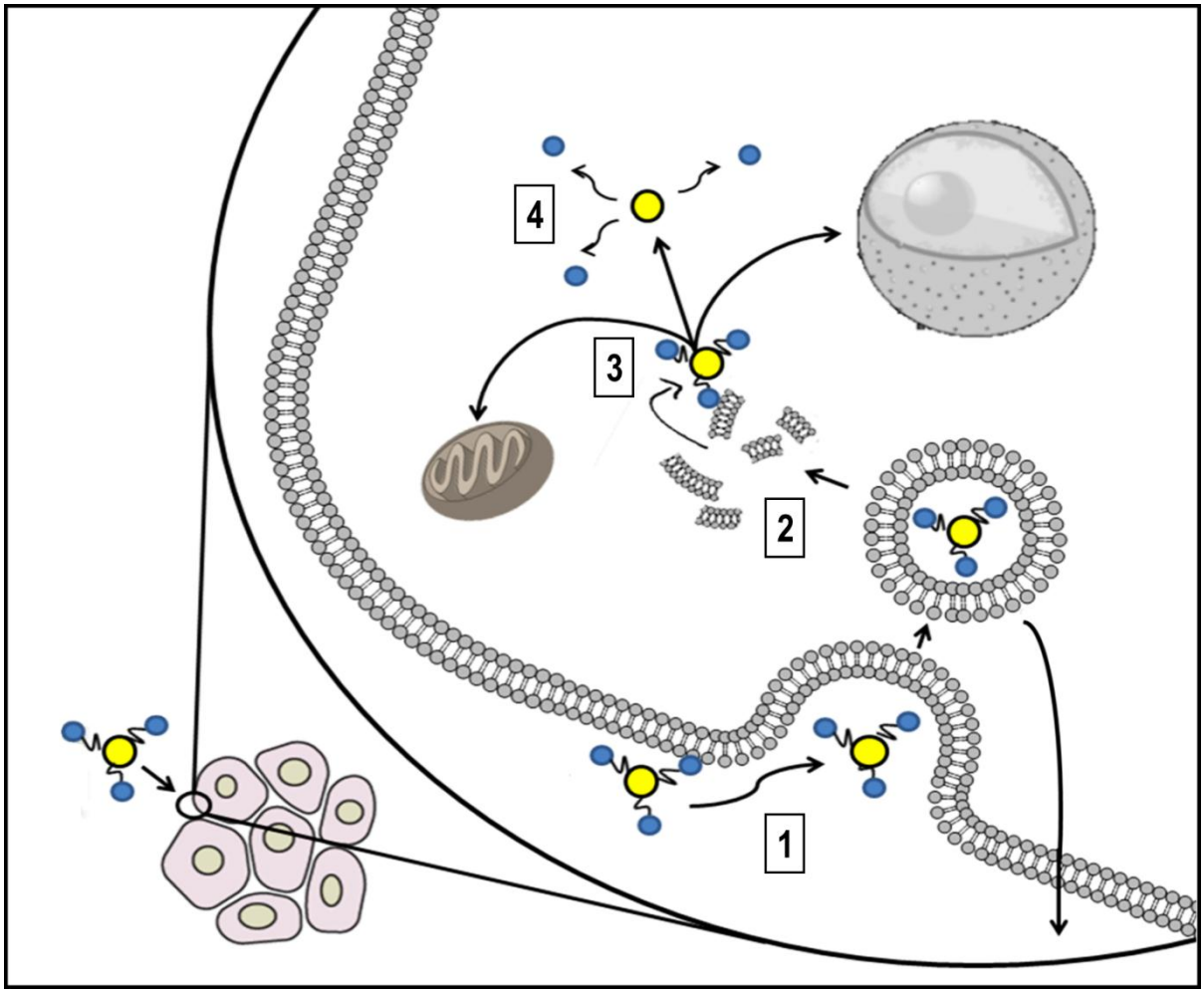

Figure 2 - Intracellular peptide delivery barriers: 1) Biomacromolecular therapeutics like peptides must first translocate the cellular membrane and become internalized in the cell 2) Once internalized, the therapeutic must escape from the endo-lysosomal pathway or consequently face degradation in lysosomes and/or trafficking for exocytosis out of the cell 3) Finally, if a drug delivery vehicle is utilized to deliver the therapeutic then the vehicle must contain an inherent mechanism to release the therapeutic in order to avoid steric hindrance of bioactivity in the cytosol. Figure adopted with permission from [29].

These colloidal drug carriers are attractive because they can be modified to be multi-functional in terms of containing targeting moieties [30], cell penetrating and/or fusogenic peptides [31, 32], and environmentally responsive ‘smart’ polymers that can facilitate escape from trafficking through the endo-lysosomal pathway [33-35]. Despite the advances made in overcoming these delivery barriers, substantial limitations still exists in terms of drug carriers that simultaneously address the key delivery

barriers of stability, cellular uptake, escape from the endo-lysosomal pathway, and an effective means to ‘un-package’ or release the desired therapeutic into the proper micro-environment.

Approach

The delivery requirements for intracellular-acting biomolecules like peptides are more rigorous because upon endocytosis, the predominant fate is enzymatic degradation in lysosomes or endosomal recycling and subsequent exocytosis from the cell. Here, we describe a novel method to form nanometer-sized electrostatic complexes that contain a therapeutic inhibitory peptide (i.e. MK2i) and a “smart” polymer component. This ‘smart’ polymer can recognize environmental changes in pH, and thus can respond to the proton pump-mediated acidification of endosomal vesicles to release the therapeutic payload while simultaneously disrupting the endosomal membrane to allow for cytosolic peptide delivery. This simple yet innovative approach to intracellular peptide delivery may enable a new level of pharmaceutical breadth and specificity that would overcome many of the drug delivery barriers that biomacromolecular drugs face, allowing for manipulation of intracellular targets that were previously considered “un-druggable”. The majority of peptide-based therapeutics solely rely on the use of a cell penetrating peptide sequence to enhance uptake, but they do not include an inherent mechanism to escape from trafficking through the endo-lysosomal pathway. Most of these cell penetrating peptides are cationic in nature and are typically rich in positively-charged amino acid residues [29], making biologic drugs containing cell penetrating peptide sequences well-suited to electrostatic complexation with anionic polymer-based carrier systems that can facilitate endosomal escape. The use of environmentally-responsive ‘smart’ polymers in conjunction with techniques to enhance cellular uptake would result in optimized payload delivery to the intracellular micro-environment where the therapeutic target is located; The innovative combination of endosomolytic “smart” polymer technology and cell penetrant peptides provides a platform for the enhanced intracellular delivery of peptide-based therapeutics for a wide range of medical applications.

Here, we introduce a robust approach for the intracellular delivery of a peptide inhibitor of MK2 to modulate VSMC phenotype. This new platform incorporates an anionic “smart” polymer that

can form electrostatic complexes with an optimized, highly-specific cationic therapeutic peptide (see **fig. 3**).

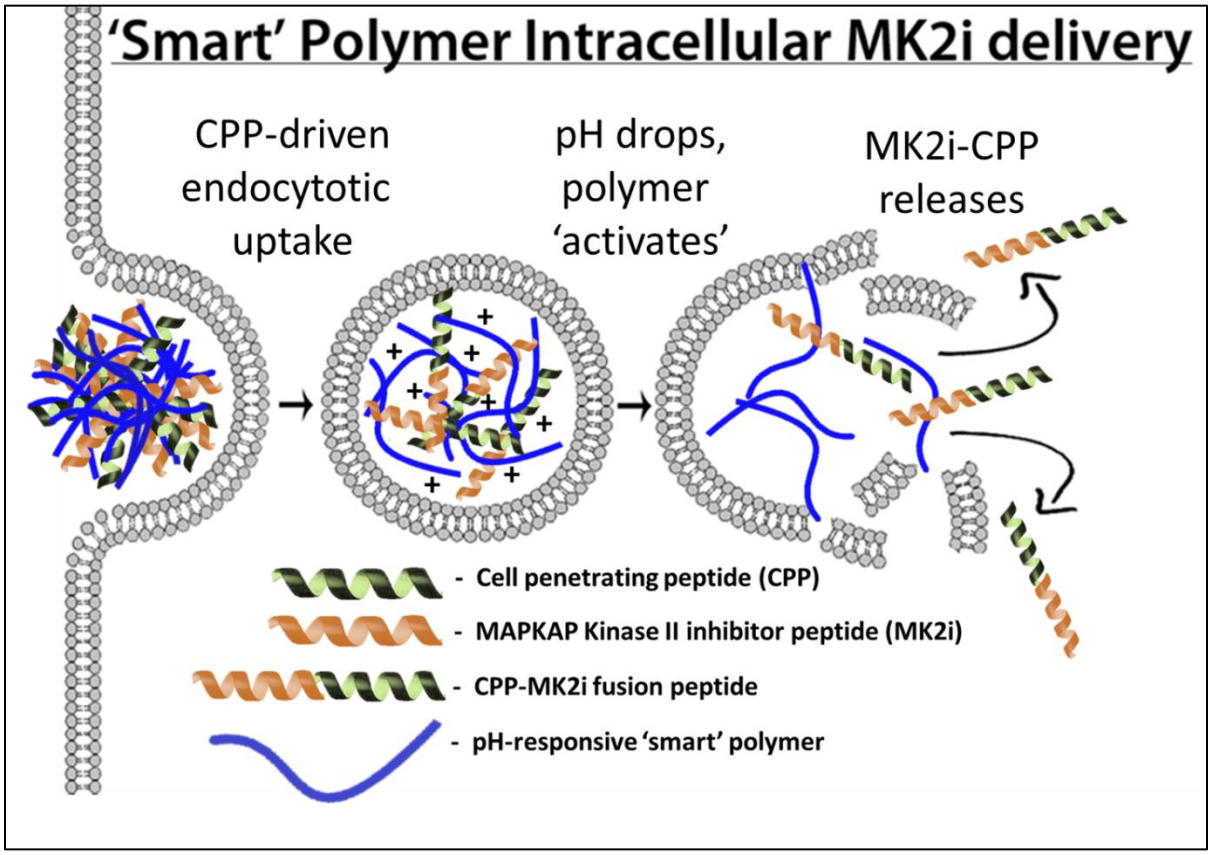

Figure 3 – Approach to achieve intracellular MK2i delivery: Nanopolyplexes composed of a cell-penetrant, cationic therapeutic peptide and an anionic 'smart' polymer that respond to the increase in acidity upon endosomal uptake to facilitate endosomal escape and release of the peptide into the cytoplasm.

CHAPTER II

ENHANCED INTRACELLULAR PEPTIDE DELIVERY WITH PH-RESPONSIVE, ENDOSOMOLYTIC NANO-POLYPLEXES TO MODULATE VASCULAR SMOOTH MUSCLE CELL BEHAVIOR

Introduction

The clinical potential of peptide-based therapeutics has increased over the past few decades, and these therapeutics continue to be extensively utilized as lead compounds in the drug discovery process to elucidate the mechanisms of molecular recognition and target-specificity [36]. Despite the advantages offered by peptide based therapeutics (biomimetic, increased target-specificity, and high potency), the shortcomings of poor bioavailability, limited membrane permeability, and metabolic instability result in a clinical preference for low-cost small-molecule drugs characterized by reduced target-specificity that can result in non-specific side effects in humans [12]. The current work focuses on development of a platform technology to be used for the enhanced intracellular delivery of therapeutic peptides to overcome these shortcomings.

An effective means to facilitate endosomal escape has been the primary limitation to the success of peptide based therapeutics in clinical applications. As aforementioned, a variety of approaches have been developed to facilitate endosomal escape, specifically pH-responsive “smart” polymers that can respond to the environment encountered in the endosomal pathway [37]. Controlled polymerization techniques, specifically reversible addition-fragmentation chain transfer (RAFT) polymerization, offer a promising approach to designing synthetic polymers that are monodisperse, and contain spatially-defined functionalities [38, 39], and these techniques can be used to synthesize well-defined, pH-responsive polymers that can be utilized as endosomolytic agents in drug delivery applications [9].

By enhancing the cytosolic delivery of intracellular-acting peptides the required dose can be minimized, reducing cost and maximizes therapeutic efficacy. Furthermore, by optimizing the bioavailability of the therapeutic peptide in the micro-environment in which it is active may also result in an increase in the duration of therapeutic efficacy [40]. Recently, the use of pH-responsive

polymers has been reported to enhance intracellular delivery of bio-macromolecular therapeutics, ranging from the intracellular delivery of pro-apoptotic peptides for anti-cancer therapies [9, 27, 29] to the enhanced vaccine performance of antigen-polymer bioconjugates [33, 41]. However, these approaches typically involve complex conjugation chemistry necessitating extra purification steps that result in high-cost and low yields. Consequently, there exists a need to develop a simplified synthetic method to synthesize pH-responsive, endosomolytic drug delivery vectors for peptide-based therapeutics.

The current study pursues a novel approach to the synthesis of endosomolytic nano-polyplexes for the intracellular delivery of cationic peptides. This work verifies the synthesis and efficacy of electrostatic complexes containing a MK2 inhibitory peptide for the modulation of VSMC phenotype and demonstrates the potential of this platform to prevent intimal hyperplasia and improve graft patency in vascular grafting applications.

Methods

Materials

All reagents were purchased from Sigma and were of analytical grade unless otherwise stated. PD10 desalting columns were purchased from GE healthcare. Diethyl propylmalonate was purchased from Alfa Aesar (Ward Hill, MA). All monomers were filtered through a basic alumina column to remove inhibitors prior to use in polymerizations. Dioxane was distilled prior to use in polymerizations. 2,2'-Azobis(2-methylpropionitrile) (AIBN) was recrystallized twice with methanol.

Synthesis of 4-cyano-4-(ethylsulfanylthiocarbonyl) sulfanylvpentanoic acid (ECT)

The RAFT chain transfer agent ECT was synthesized following protocols previously described by Convertine et al. [42] and adapted from Moad et al. [43]. Briefly, Ethanethiol (76 mmol, 4.72 g) was reacted with carbon disulfide (79 mmol, 6.0 g) in the presence of sodium hydride (79 mmol, 3.15 g) in diethyl ether for 1h. The resulting sodium S-ethyl trithiocarbonate was further reacted with iodine (25 mmol, 6.3 g) to obtain bis(ethylfulfanyl-thiocarbonyl) disulfide, which was further

refluxed with 4,4'-azobis(4-cyanopentanoic acid) in ethylacetate for 18 h. The crude ECT was purified by column chromatography using silica gel as the stationary phase and a gradient of ethyl acetate:hexane (40:60 to 70:30) as the mobile phase. ^{1}H NMR (400MHz, $CDCl_3$): δ 1.36 t ($SCH_2C\mathbf{H}_3$); δ 1.88 s ($CCNC\mathbf{H}_3$); δ 2.3–2.65 m ($C\mathbf{H}_2C\mathbf{H}_2$); δ 3.35 q ($SC\mathbf{H}_2CH_3$).

Synthesis of 2-propylacrylic acid (2-PAA)

The synthesis of PAA was adapted from existing methods developed by Ferrito et al. [44]. Briefly, diethyl propylmalonate (200 mmol, 40.45 g) was stirred in 1M KOH in 95% ethanol and acidified with HCl to yield 2-carbopropoxybutyric acid, which was reacted with diethylamine (200 mmol, 14.62 g) and formalin (200 mmol, 16.11 g) at room temperature for 24h, followed by reflux at 60°C for 8 hours. Following acidification with sulfuric acid, the resulting 2-propylacrylate was extracted 3x with diethyl ether and dried over magnesium sulfate. The pure 2-propylacrylate was then refluxed in 2M KOH for 20 h to yield 2-propyl acrylic acid, which was extracted 3x with diethyl ether, dried, and vacuum distilled under vacuum to yield a colorless oil. ^{1}H NMR (400 MHz, $CDCl_3$) δ 0.97 t ($C\mathbf{H}_3CH_2$); δ 1.55 m ($CH_3C\mathbf{H}_2CH_2$); δ 2.31 t ($CH_3CH_2C\mathbf{H}_2$); δ 5.69-6.32 q ($C\mathbf{H}_2$=C); δ 12 s (CCOO**H**).

Synthesis and Characterization Poly(propylacrylic acid) (PPAA) and Poly(acrylic acid) (AA)

The ECT chain transfer agent (CTA) was utilized in the RAFT polymerization of a poly(2-propylacrylic acid) homopolymer (PPAA) that was carried out in bulk under a nitrogen atmosphere at 70°C for 48 hours using AIBN as the free radical initiator. The reaction mix was put through three freeze-vacuum-thaw cycles and purged with nitrogen for thirty minutes prior to polymerization. The molar ratio of CTA to AIBN was 1 to 1 and the monomer to CTA ratio was set so that a molecular weight of 25,000 g/mol would be achieved at 100% conversion. Following polymerization, the resultant polymer was dissolved in DMF and precipitated into ether 5 times before drying overnight *in vacuo*. The RAFT polymerization of a poly(acrylic acid) homopolymer (AA) was carried out in distilled dioxane under a nitrogen atmosphere at 70°C for 18 hours using AIBN as the free radical initiator and ECT as the CTA. The reaction mix was purged with nitrogen for thirty minutes prior to polymerization. The molar ratio of CTA to AIBN was 5 to 1 and the monomer to CTA ratio was set so that a molecular

weight of 8,000 g/mol would be achieved at 100% conversion. Following polymerization, the resultant polymer was dissolved in dioxane and precipitated into ether 5 times before drying overnight *in vacuo*. Gel permeation chromatography (GPC, Agilent) was used to determine molecular weight and polydispersity (M_w/M_n, PDI) of the PPAA and AA homopolymers using HPLC-grade DMF containing 0.1% LiBr at 60°C as mobile phase. Molecular weight calculations were calculated with ASTRA V software (Wyatt Technology) and were based on calculated dn/dc values for PPAA determined through injection of serial dilutions of the polymer in conjunction with off-line refractive index monitoring (calculated PPAA dn/dc = 0.087 mL/g, calculated PAA dn/dc = 0.09 mL/g).

Synthesis of YARA-MK2i and YARA Peptides

A cell penetrant MK2 inhibitor peptide (YARA-MK2i, sequence YARAAARQARA-KALARQLGVAA MW = 2283.67) and a control cell penetrating peptide (YARA, sequence YARAAARQARA MW = 1204.37) were synthesized on a PS3 3 channel serial peptide synthesizer (Protein Technologies, Inc. Tucson, AZ) utilizing standard Fmoc Chemistry. N-methylpyrrolidone (NMP, Fischer Scientific) was utilized as a solvent in all peptide syntheses. HCTU was used as an activator (Chempep, Wellington, FL) in the presence of N-methylmorpholine. All amino acids were double coupled in order to maximize yield and purity. Peptides were cleaved/deprotected in Reagent B: TFA/Phenol/H_2O/triisopropylsilane (88/5/5/2). Successful peptide synthesis was verified through LC-MS analysis on a Waters Synapt ESI-MS. Peptides were then further purified by reverse phase HPLC on a Waters 1525 binary HPLC pump outfitted with an extended flow kit, a Waters 2489 UV/Visible detector and a phenomenex Luna C18(2) AXIA packed column (100A, 250 x 21.2 mm, 5 micron). **A)** HPLC grade water with 0.05% formic acid and **B)** HPLC grade acetonitrile were used as the mobile phases and the peptide was purified utilizing a 90% A to 100% B gradient over 25 minutes (16 mL/min). Acetonitrile was removed from purified fractions with a rotary evaporator and the purified fractions were then frozen, lyophilized, and peptide purity was verified through electrospray ionization mass spectrometry (ESI-MS).

Synthesis and Characterization of Polyplexes

Poly(propylacrylic acid) was dissolved in 1 M NaOH and diluted into a phosphate buffer (pH 8) to obtain a stock solution. Purified YARA-MK2i peptide was dissolved in phosphate buffer (pH 8). The defined pH of the stock solutions was selected as an optimal balance between the pKa values of the primary amines present on the YARA-MK2i peptide (i.e. NH_3^+, pKa ~ 9-12 depending on amino acid) and the pKa values of the carboxylic acid moieties present on the polymer backbone (i.e. COO^-, pKa ~ 6.7). The YARA-MK2i peptide and PPAA polymer were mixed at a range of charge ratios ($[NH_3^+]/[COO^-]$) from 10:1 to 1:10 to form polyplexes (see **fig. 4)**. The resulting polyplexes were syringe filtered through 0.45 μm PTFE filter and the hydrodynamic radius and ζ-potential were characterized by dynamic light scattering (DLS) analysis in a Malvern zetasizer Nano-ZS with a reusable dip cell kit (Malvern Instruments Ltd., Worcestershire, U.K.).

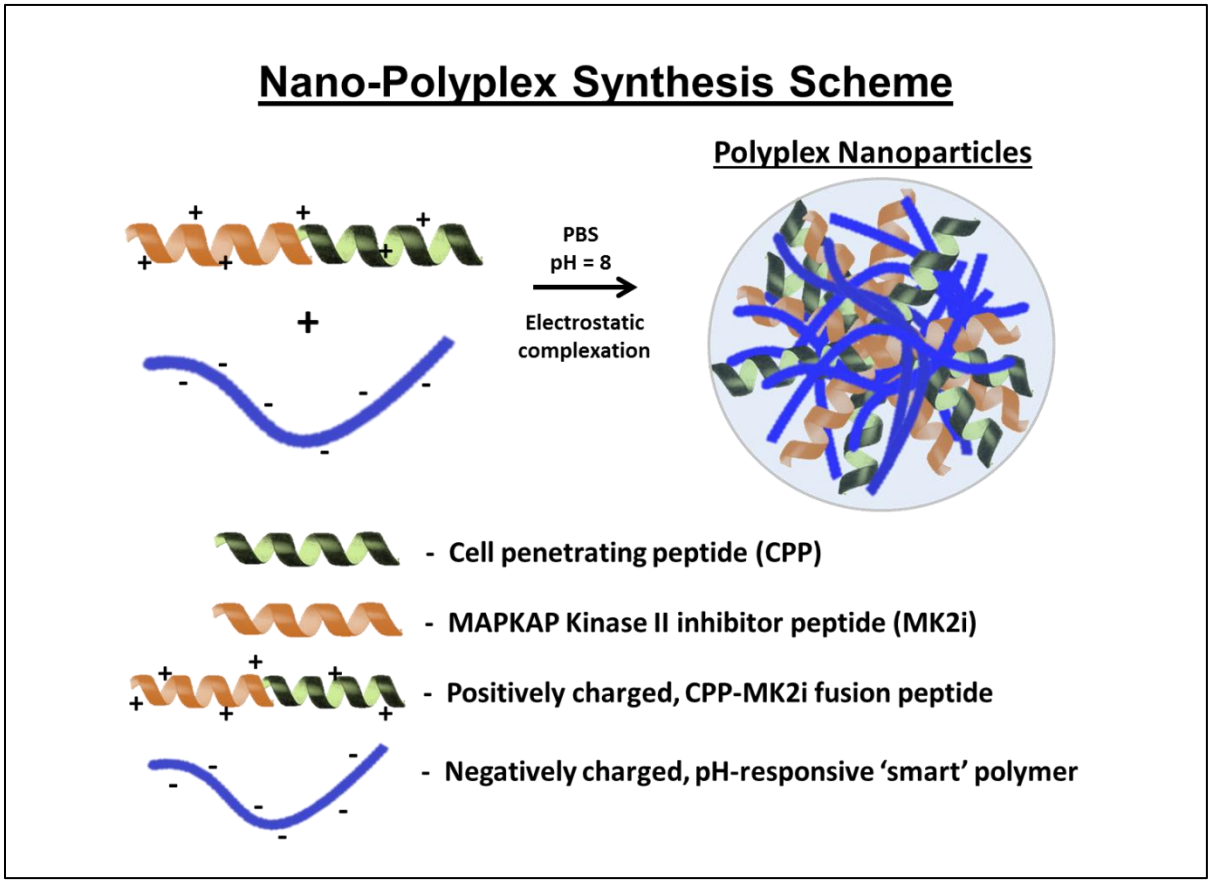

Figure 4 – Polyplex nanoparticle synthesis scheme: Mixing the YARA-MK2i fusion peptide and pH-responsive, endosomolytic polymer at the appropriate pH (between the pKa

values of the primary amines present on the peptide and the carboxylic acid groups present in the polymer) results in the formation of electrostatic complexes, or 'polyplex' nanoparticles. A CR of 1:3 was then chosen as the optimal formulation and used in subsequent cell studies.

In order to verify the sizes indicated by DLS analysis, polyplexes at a charge ratio of 1:3 were visualized through transmission electron microscopy (TEM) imaging. TEM samples were prepared by inverting carbon film-backed copper grids (Ted Pella) onto a 20 µL droplet of aqueous polyplex suspensions (1 mg/mL) and blotted dry. All samples were then inverted onto a 20 µL droplet of 3% Uranyl Acetate and allowed to stain for 2 min. After blotting the sample dry, samples were desiccated *in vacuo* for 2 h prior to imaging on a Philips CM20 system operating at 200 kV. Images were collected using a CCD camera with AMT Image capture Engine software (Advanced Microscopy Techniques, Danvers, MA). PH-dependent size changes of polypexes at a CR of 1:3 were then quantified by DLS analysis at various pH values (i.e. pH 7.4, 6.8, 6.2, and 5.6).

PH-Dependent Membrane Disruption Hemolysis Assay

In order to assess the polyplexes' potential for enhancing endosomal escape, a red blood cell hemolysis assay was utilized as previously described [45] to measure the capacity of polyplexes to cause pH-dependent disruption of lipid bilayers. Briefly, following approval by Vanderbilt Medical Center's Institutional Review Board, whole human blood from an anonymous donor was drawn and plasma was aspirated following centrifugation of the red blood cells. The remaining erythrocytes were washed three times with 150 mM NaCl and re-suspended into phosphate buffers corresponding to physiologic (pH 7.4), early endosome (pH 6.8), early/late endosome (pH 6.2), and late endosome/lysosomal (pH 5.8) environments. The polyplexes and peptides (1-40 µg/mL), PBS (negative control), or 1% Triton X-100 (positive control) was added to the erythrocyte suspensions and incubated at 37 °C for 1 hour. Intact erythrocytes were pelleted via centrifugation, and supernatant was carefully transferred to a new 96-well plate. The hemoglobin content within the supernatant was then measured via absorbance at 541 nm. Percent hemolysis was determined relative to Triton X-100 and PBS controls.

Cell Culture

Primary human coronary artery vascular smooth muscle cells (HCAVSMCs) were obtained from Lonza; HCAVSMCs were cultured in Vascular cell basal medium (ATCC) supplemented with 5% FBS, human basic fibroblast growth factor (bFGF, 5 ng/mL), human Insulin (5µg/mL), Ascorbic acid (50 µg/mL), L-glutamine (10 mM), and human epidermal growth factor (EGF, 5 ng/mL), and 1% penicillin-streptomycin.

All cultures were maintained in 75cm^2 polystyrene tissue culture flasks at 37°C, 5% CO_2 environment with cell culture media refreshed every other day. All cells were seeded at a density of 20,000-40,000 cells/cm^2, as required by the specific experiment, and allowed to grow to 80-90% confluence prior to being harvested/passaged. Only cells from early passages (numbers 3-7) were used in experiments.

Polyplex Cytotoxicity

The CytoTox-ONE Homogenous Membrane Integrity assay (Promega) was used to assess the cytotoxicity of peptide and polyplex treatments according to the manufacturer's instructions. Briefly, HCAVSMCs from early passage were grown to 80-90% confluence in a 75 cm^2 tissue culture flask in a 37°C/5% CO_2 incubator prior to harvest. 200 µL of cell suspension (at 10,000 cells/well) was seeded onto 96-well plates to yield an approximate 70% confluence per well. Cells were allowed to adhere to the plate overnight. Cells were treated with polyplexes or peptides alone and incubated for 2 hours. Following treatment, cells were aspirated and 200 µL of fresh medium was added to each well. After 24 hours of incubation in fresh media cells were washed 2x with PBS and re-suspended in 100 µL lysis buffer. Each well was then supplemented with 100 µL Lactate dehydrogenase (**LDH**) substrate and incubated at RT for 10 minutes prior to the addition of 50 µL stop solution. LDH-induced fluorescence (excitation 550 nm, emission 600 nm) was then quantified with a TECAN Infinite M1000 Pro plate reader and used to determine cell viability compared to untreated control groups.

Inflammatory Cytokine Analysis

In order to evaluate the ability of polyplexes to inhibit Interleukin-6 production, HCAVSMCs were cultured and seeded onto a 96-well plate using the methods described in the LDH cytotoxicity assay above. Cells were treated with 20 ng/mL tumor necrosis factor-α (**TNFα**) for 4 hours followed by treatment with polyplexes or peptides alone for 2 hours. Following treatment, each well was aspirated and supplemented with fresh medium. After 12 and 24 hours, 100 µL of supernatant was collected and frozen at -80°C until cytokine analysis could be performed.

Similarly, to evaluate the ability of polyplexes to inhibit TNFα production, HCAVSMCs were cultured and seeded onto a 96-well plate using the methods described in the LDH cytotoxicity assay above. Cells were treated with 10 µM ANG II for 4 hours followed by treatment with polyplexes or peptides alone for 2 hours. Following treatment, each well was aspirated and supplemented with fresh medium. After 12 and 24 hours, 100 µL of supernatant was collected and frozen at -80°C until cytokine analysis could be performed.

Human IL-6 (cat # 900-K16) and Human TNFα (cat # 900-K25) ELISA development kits (Peprotech; Rocky Hill, NJ) were used to measure cytokine levels in supernatant collected from treated cells. For both assays 9 standards were prepared according to the manufacturer's protocol. 40 µL of supernatant was diluted with 60 µL diluent; quadruplicates of each sample were used. Absorbance at 405 nm with wavelength correction at 650 nm was monitored for 1 hour with readings taken every 5 minutes. Concentrations of IL-6 and TNFα were determined through extrapolation from a 4 parameter logistic fit of the standard curve. All data were then normalized to cell viability determined through a LDH-based cytotoxicity assay. Data are expressed as mean ± SEM.

Microscopic Analysis of Cellular Uptake and Trafficking

An amine-reactive 5(6) carboxyfluorescein succinimidyl ester was dissolved in DMSO and mixed at a 1 to 1 molar ratio with the YARA-MK2i peptide in 100 mM sodium bicarbonate buffer (pH = 8.3). Unreacted fluorophore and organic solvent were removed using a PD-10 miditrap G-10 desalting column, and the fluorescently labeled peptide was lyophilized. After accounting for the loss of a primary amine from the peptide due to conjugation of the fluorophore, PPAA polymer or AA polymer and fluorescently labeled YARA-MK2i peptide were mixed at a CR of $[NH_3^+]/[COO^-]$ = 1:3 to

form polyplexes and syringe filtered through a 0.45 µm PTFE filter. Fluorescent polyplex size and zeta potential were measured by DLS analysis. Fluorescently-labeled peptide alone or fluorescent polyplexes were applied to HCAVSMCs grown on 8-well chambered microscope slides at a concentration of 25 µM YARA-MK2i or YARA in DMEM media supplemented with 1% FBS and 1% P/S. Cells were pre-incubated in low serum growth media for 24 hours to cause quiescence. Cells were then treated in quadruplicate for 2 hours, washed with PBS -/-, and the medium was refreshed. Cells were then incubated for an additional 0, 2, 10, or 22 hours. For the final two hours of incubation or treatment 50 nM Lysotracker Red DND-99 was added to each well in order to visualize acidic endo/lysosomal vesicles within cells. After incubation, cells were washed with 0.1% trypan blue for 1 minute to quench extracellular fluorescence followed by 2 additional washes with PBS -/-. Cells were then imaged using a LSM 710 META fluorescence microscope with ZEN imaging software (Carl Zeiss Thornwood, NY).

All images were processed using ImageJ and Mander's coefficients for quantifying co-localization were calculated using Just Another Colocalization Plugin (JACoP) [46]. Mander's coefficients calculated from 3 separate images for each treatment group were averaged to obtain average colocalization values. Pixel intensity thresholds were set for both the green (fluorescein) and red (lysotracker) channels so that background pixels were excluded form colocalization calculations.

Flow Cytometric Quantification of Cellular Uptake and Intracellular Peptide Half-life

HCAVSMCs were grown to 80-90% confluence, harvested, and seeded at 40,000 cells/mL in a 24 well tissue culture plate. Fluorescent YARA-MK2i and polyplexes were synthesized as noted above in the microscopic analysis of cellular uptake section and HCAVSMCs were quiesced in low serum growth media (1% FBS, 1% P/S in DMEM) for 24 hours to ensure that cellular uptake and retention was not affected by actively proliferating cells. Cells were then treated in triplicate with fluorescently-labeled peptide alone or fluorescent polyplexes at a concentration of 25 µM YARA-MK2i for 2 hours, washed with PBS -/-, and the medium was refreshed. Cells were then incubated for an additional 0, 2, 10, 22, or 46 hours. Cells were then washed with PBS -/-, trypsinized, and re-suspended in 0.1% Trypan blue in PBS (-/-) for flow cytometric analysis on a BD (Franklin Lakes, NJ)

FACSCalibur system utilizing BD Cellquest Pro (version 5.2) acquisition software. The FL1 channel (emission filter at 530 ± 15 nm) was used to quantify the FAM-based fluorescence from each cell. Average fluorescence intensities for each time point were averaged and a half-life for intracellular fluorescence was calculated by fitting an exponential curve to the data.

Statistical Analysis

Statistical analysis was performed with one-way ANOVA followed by a Tukey test to compare experimental groups. Analyses were done with Minitab 16 software (State College, PA) or Microsoft Excel. Statistical significance was accepted within a 95% confidence limit. Results are presented as arithmetic mean ± SEM graphically.

Results

Polymer Synthesis and Characterization

4-cyano-4-(ethylsulfanylthiocarbonyl) sulfanylvpentanoic acid (ECT) was synthesized as previously described [Convertine, 2009 #34]. 2-propyl acrylic acid (PAA) was synthesized using established methods [Ferrito M, 1992 #36]. RAFT polymerization was used to synthesize a poly(propylacrylic acid) homopolymer [PPAA, M_n = 22,010 g/mol, PDI = 1.47 (GPC) **Appendix A**]. ^{1}H-NMR was used to verify molecular weight determination yield by GPC analysis (M_n = 21,950, **Appendix B**). Similarly, RAFT polymerization was used to synthesize a poly(acrylic acid) homopolymer (**AA**) with a targeted molecular weight of 8,000 g/mol [M_n = 10,830, PDI = 1.27 (GPC) **Appendix A**] and molecular weight determined by GPC was verified by ^{1}H-NMR (M_n = 7,640, **Appendix B)**.

Peptide Synthesis and Purification

The Purity of the HPLC-Purified YARA-MK2i and YARA peptides was verified through electrospray ionization mass spectrometry (YARA-MK2i MW = 2283.67 g/mol, YARA MW = 1204.37 **figs. 5A-B**).

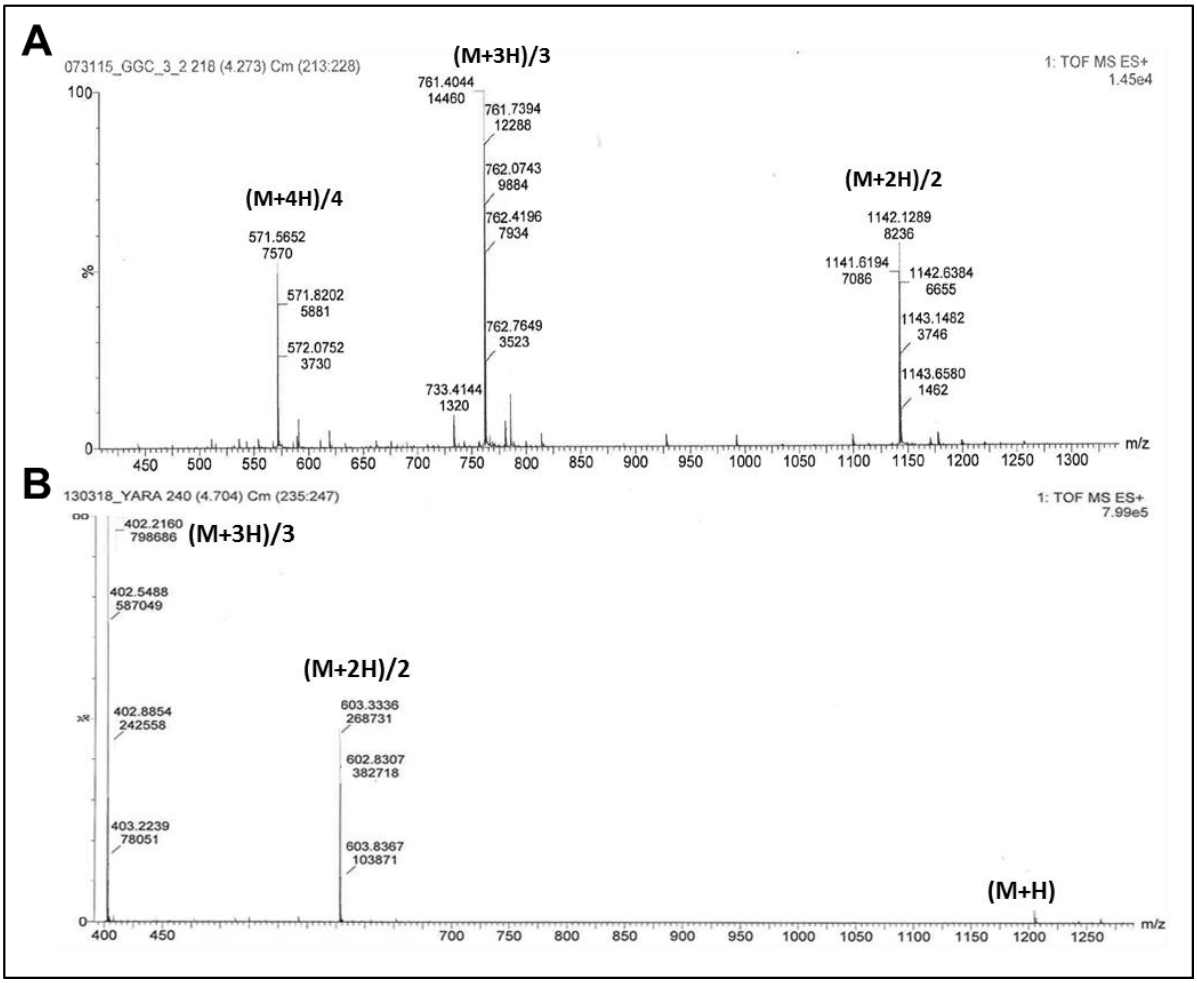

Figure 5 – YARA-MK2i and YARA Mass Spectra: Electrospray-ionization mass spectrometry (ESI-MS) mass spectrum for **A)** the HPLC-purified YARA-MK2i fusion peptide (sequence: YARAAARQARA-KALARQLGVAA, MW = 2283.67 g/mol) and **B)** the YARA cell penetrating peptide (sequence: YARAAARQARA, MW = 1204.37 g/mol). Each spectrum shows multiple peaks, all of which correspond to the full peptide weight.

Polyplex Synthesis and Characterization

Polyplexes were formed by mixing the pH-responsive PPAA polymer with the YARA-MK2i peptide in a buffered solution with a defined pH between the pKa values of the carboxylic acid groups and primary amines present on the polymer and peptide, respectively (pH 8). The polymer and peptide were mixed at a range of charge ratios from $[NH_3^+]/[COO^-]$ = 10:1 to $[NH_3^+]/[COO^-]$ = 1:10. DLS analysis revealed that the charge ratio significantly affected polyplex formation in terms of size and zeta potential, with only a narrow range of charge ratios yielding a unimodal size distribution of

nanoparticles (i.e. charge ratios of 1:2 and 1:3, see **fig. 6A**). It should also be noted that a visible precipitate formed upon mixing at charge ratios between $[NH_3^+]/[COO^-]$ = 2:1 to 1:1.5. After considering the size distribution for all formulations, a charge ratio of 1:3 was chosen as the optimal formulation as this ratio consistently yielded a unimodal size distribution with minimal particle size and polydispersity (hydrodynamic diameter = 118.8.9 ± 26.76 nm, ζ = -11.9 ± 3.18 mV). Furthermore, fluorescent polyplexes prepared with a fluorescently-labeled YARA-MK2i peptide and control polyplexes formulated with the YARA cell penetrating peptide alone (subsequently herein referred to as CPP polyplexes), both at a charge ratio of 1:3, yielded similar size distributions to the YARA-MK2i polyplexes. As expected, the ζ-potential decreased as the ratio of polymer to peptide increased, with a charge ratio of $[NH_3^+]/[COO^-]$ = 2:1 yielding a near neutral ζ-potential (see **fig. 6B**). Furthermore, both the fluorescently labeled polyplexes and the control CPP polyplexes were found to have similar ζ-potentials to the YARA-MK2i polyplex at a charge ratio of 1:3.

A

NH2:COOH	Z-ave diameter (nm)	PDI
10:1	10.32 ± 2.63*	0.314
2:1	52.1 ± 46.86*	0.297
1:1	970.6 ± 662.4	0.41
1:1.5	465.1 ± 138.4*	0.5465
1:2	474.2 ± 32.59	0.239
1:3	118.8 ± 26.76	0.271
1:4	607.4 ± 285.2*	0.662
1:5	213.0 ± 67.95*	0.407
1:10	21.57 ± 9.89*	0.355
1:3 (FAM)	158 ± 56.67	0.308
1:3 (CPP)	126.6 ± 22.31	0.248
1:3 (AA)	113.7 ± 14.47	0.577
1:3 (AA-FAM)	236.5 ± 69.74	0.522

B

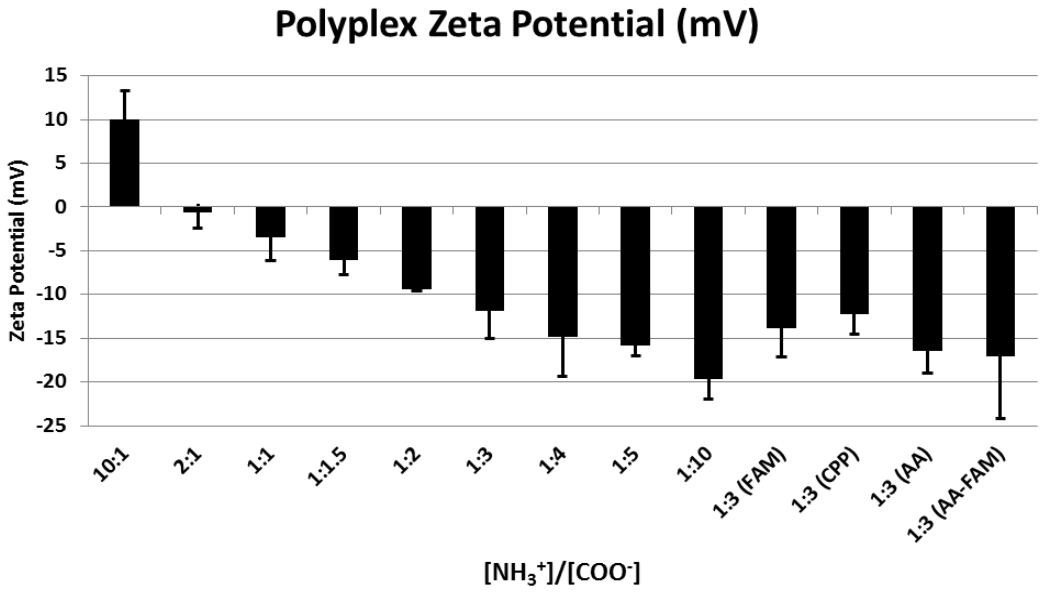

Figure 6 – Polyplex characterization summary: A) Table of the sizes of polyplexes prepared at different charge ratios ($[NH_3^+]/[COO^-]$) determined by DLS analysis. Asterisks (*) indicate size distributions with multiple peaks present. 1:3 (FAM) polyplexes were formulated with a carboxyfluorescein fluorophore-labeled YARA-MK2i peptide to use in cellular uptake studies. 1:3 (CPP) polyplexes were formulated with the cell penetrating peptide sequence YARA (i.e. no therapeutic MK2 inhibitory peptide) to use as a peptide control. 1:3 (AA) polyplexes were formulated with an acrylic acid polymer that does not have a pH response in the desired pH range as a vehicle control. **B)** ζ-potential of polyplexes prepared at different charge ratios ($[NH_3^+]/[COO^-]$) determined on a Zetasizer Nano ZS. Values shown are an average of at least 3 independent measurements.

In order to verify the DLS results, uranyl acetate-stained polyplexes (at a charge ratio = 1:3) were imaged using transmission electron microscopy. TEM images revealed particle sizes in agreement with results from DLS analysis (see **fig. 7A-C**).

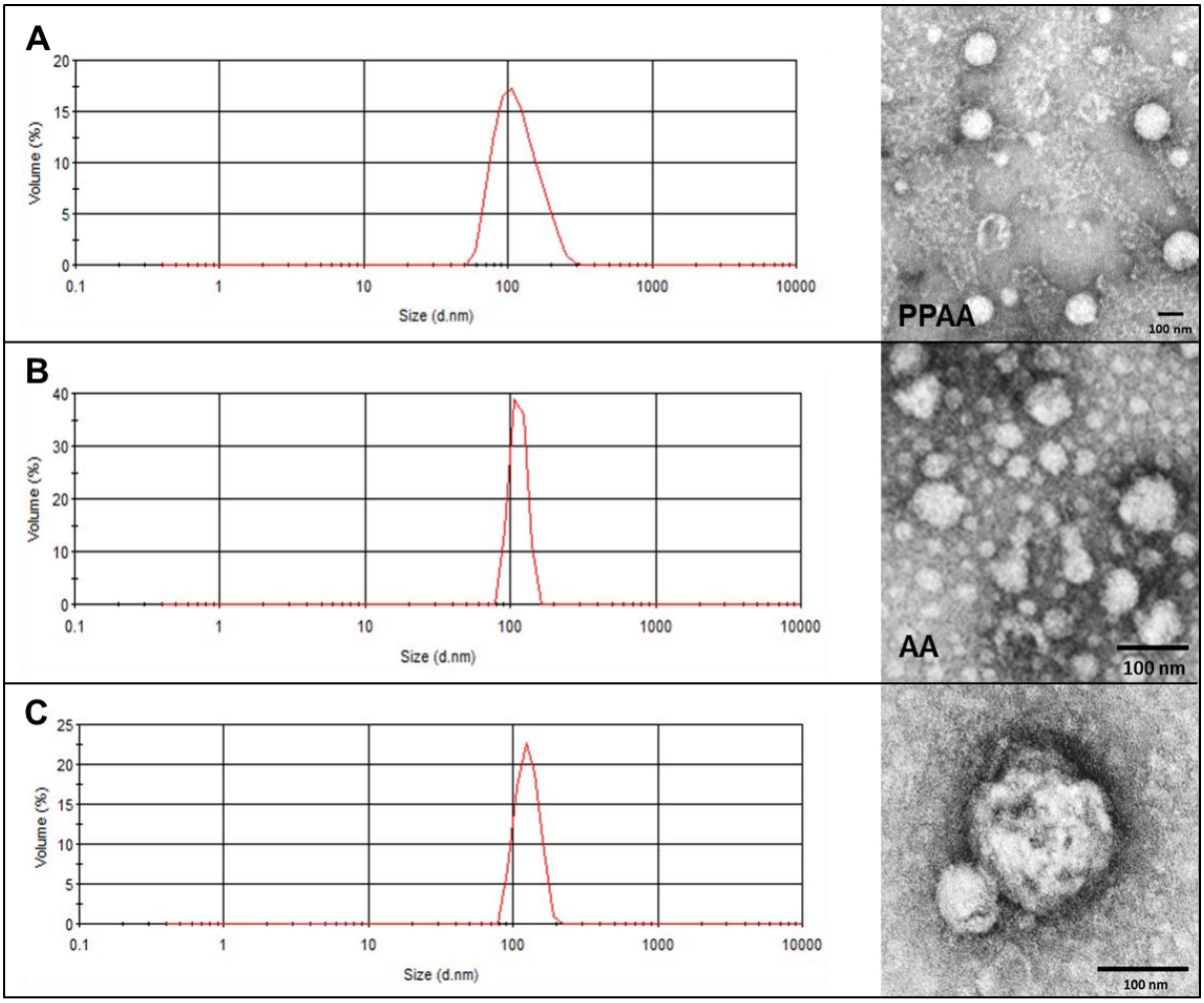

Figure 7 – DLS and TEM analysis of polyplex morphology: Size distribution and representative TEM images of **(A)** PPAA polyplexes, **(B)** AA polyplexes, and **(C)** CPP polyplexes. All polyplexes were prepared at a charge ratio of $[NH_3^+]/[COO^-]$ = 1:3 (Scale bars = 100 nm).

In order to verify that the pH-responsive behavior of the PPAA polymer is maintained when electrostatically complexed with the CPP-MK2i peptide the pH-dependent size changes of polyplexes at a charge ratio of 1:3 were measured by DLS. Results indicate that as the pH approaches the pKa value (6.7) of the carboxylic acid groups on the PPAA polymer that these groups become protonated, resulting in neutralization of the polymer and cationic, electrostatic repulsion of the peptide and

subsequent dissociation of the polyplex into polymer and peptide unimers (see **fig. 8B-E**). Red blood cell hemolysis was used to measure pH-dependent membrane disruption activity of polyplexes at pH values mimicking physiologic (pH 7.4), early endosome (pH 6.8), early/late endosome (pH 6.2), and late endosome/lysosomal (pH 5.8) environments (see **fig. 8A**). At physiologic and even early endosomal pH, no significant red blood cell membrane disruption was observed even at polymer concentrations as high as 40 μg/mL. However, as the pH was lowered to late endosomal values, a significant increase in hemolysis was observed, with greater membrane disruption at pH 5.8 compared to 6.6. The hemolytic behavior of the polymer was directly proportional to polymer concentration, with over 90% erythrocyte lysis occurring at 40 μg/mL polymer in pH 5.8 buffer. This switch-like transition to a membrane disruptive conformation at late endosomal pH combined with negligible membrane disruptive activity in the physiologic pH range demonstrates the desired functionality of the polyplexes and further indicates their potential as non-toxic, endosomolytic intracellular delivery vehicles. Interestingly, the polyplexes demonstrated less hemolytic capacity than the pH responsive polymer alone, indicating that the formation of an electrostatic complex with the YARA-MK2i peptide slightly masks the membrane-disruptive activity of the polymer. This finding is consistent with the pH-dependent size changes monitored by DLS, which evinced polyplex dissociation at early endosomal pH values (i.e. pH 6.8), indicating that as the endosomal pH decreases the polyplexes will first dissociate and subsequently disrupt the endosomal membrane. This behavior is advantageous in that it effectively “un-packages” the therapeutic peptide from the electrostatic complexes prior to cytoplasmic release, ensuring that peptide bioactivity is not hindered due to steric hindrance from the pH-responsive polymer.

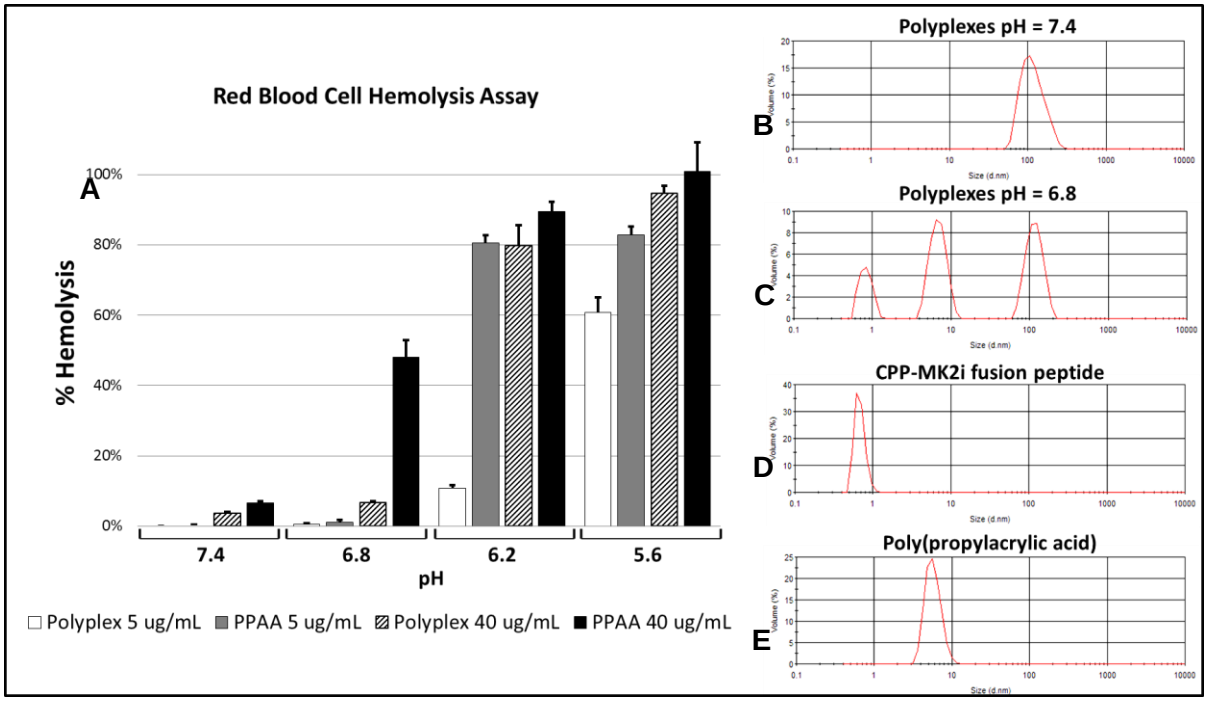

Figure 8 – Polyplex pH-responsive behavior: (A) PH-dependent hemolysis of polyplexes prepared at a charge ratio of $[NH_3^+]/[COO^-]$ = 1:3. Significant hemolysis was demonstrated at pH values representative of early to late endosomal vesicles (i.e. pH < 6.8), whereas no significant hemolysis was seen at a physiologic pH of 7.4. AA polyplexes did not show any significant hemolysis at any pH value tested (data not shown). PH-dependent size changes of polyplexes prepared at a charge ratio of $[NH_3^+]/[COO^-]$ = 1:3 were analyzed through DLS analysis. **(B)** Polyplexes at PH 7.4 show a unimodal size distribution. **(C)** Upon decreasing pH polyplexes begin to dissociate into individual fusion peptide and polymer unimers as shown in **(D)** and **(E)** respectively.

In Vitro Analysis of Polyplex Biocompatibility and Bioactivity

In order to assess the *in vitro* therapeutic efficacy and cytocompatibility of polyplexes compared to the CPP-MK2i peptide alone, TNFα and ANG II-stimulated HCAVSMCs were treated with a range of polyplex and peptide concentrations for 2 hours and incubated in fresh media for 24 hours. Following incubation, supernatant was collected for cytokine analysis and an LDH assay was used to quantify cell viability. Polyplexes showed no significant toxicity except in TNFα-stimulated HCAVSMCs at the highest concentration tested (**Appendix C**). Furthermore, polyplexes formulated with the YARA cell penetrating peptide alone demonstrated significantly more toxicity than the YARA-MK2i polyplexes in both TNFα and ANG II-stimulated HCAVSMCs.

An enzyme-linked immunosorbent assay was performed on collected supernatants to quantify interleukin-6 (IL-6) secretion and TNFα production in TNFα and ANG II-stimulated

HCAVSMCs, respectively. Both IL-6 and TNFα are inflammatory cytokines that are activated downstream of MK2 and, thus, provide indirect measure of MK2 inhibition [6, 47, 48]. Polyplexes were found to significantly inhibit IL-6 secretion in TNFα-stimulated HCAVSMCs at all concentrations in a dose-dependent manner compared to the untreated control (see **fig. 9**). Polyplexes were also found to significantly enhance YARA-MK2i-mediated inhibition of IL-6 compared to the YARA-MK2i peptide alone at concentrations of 10 and 100 μM. Furthermore, polyplexes without the therapeutic MK2i sequence did not reduce IL-6 secretion compared to the untreated control, indicating that the enhanced inhibition of IL-6 by polyplexes is mediated by enhanced delivery of the therapeutic MK2i peptide sequence.

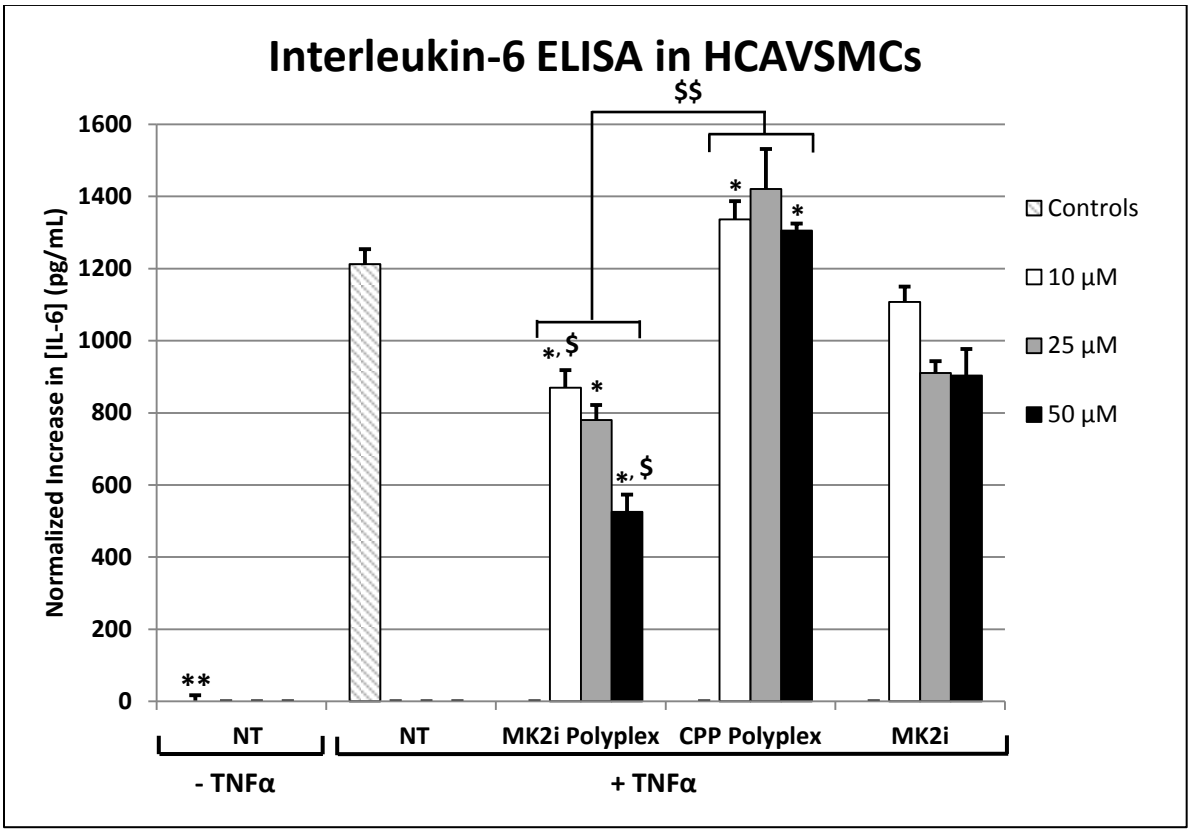

Figure 9 – Polyplex-mediated inhibition of IL-6 production: Increase in IL-6 production (compared to untreated control) in HCAVSMCs stimulated with TNFα for 6 hours, treated for two hours with polyplexes (containing the YARA-MK2i sequence or the YARA CPP alone) or the YARA-MK2i peptide alone and cultured for 24 hours in fresh media. All data is normalized to cell number as determined by an LDH assay. NT = no treatment. *$p<0.05$ compared to NT + TNFα group, **$p<0.01$ compared to NT + TNFα group, $^{\$}$ $p<0.05$ compared to MK2i at the same concentration, $^{\$\$}$ $p<0.05$ compared to CPP polyplexes at the same concentration, $n = 4$.

Polyplexes were also found to significantly inhibit TNFα secretion in ANG II-stimulated HCAVSMCs at all concentrations in a dose-dependent manner (see **fig. 10**). Measurement of TNFα secretion in ANG II-stimulated HCAVSMCs proved to be a more robust readout of polyplex activity relative inhibition of IL-6 production in response to TNFα. Polyplexes demonstrated significantly more YARA-MK2i-mediated inhibition of TNFα compared to the YARA-MK2i peptide alone at all concentrations, with a 10 μM dose of polyplex having the equivalent inhibitory effect of 100 μM YARA-MK2i peptide alone. Furthermore, polyplexes made with a poly(acrylic acid) as a vehicle control did not demonstrate any enhancement in YARA-MK2i mediated inhibition of TNFα production.

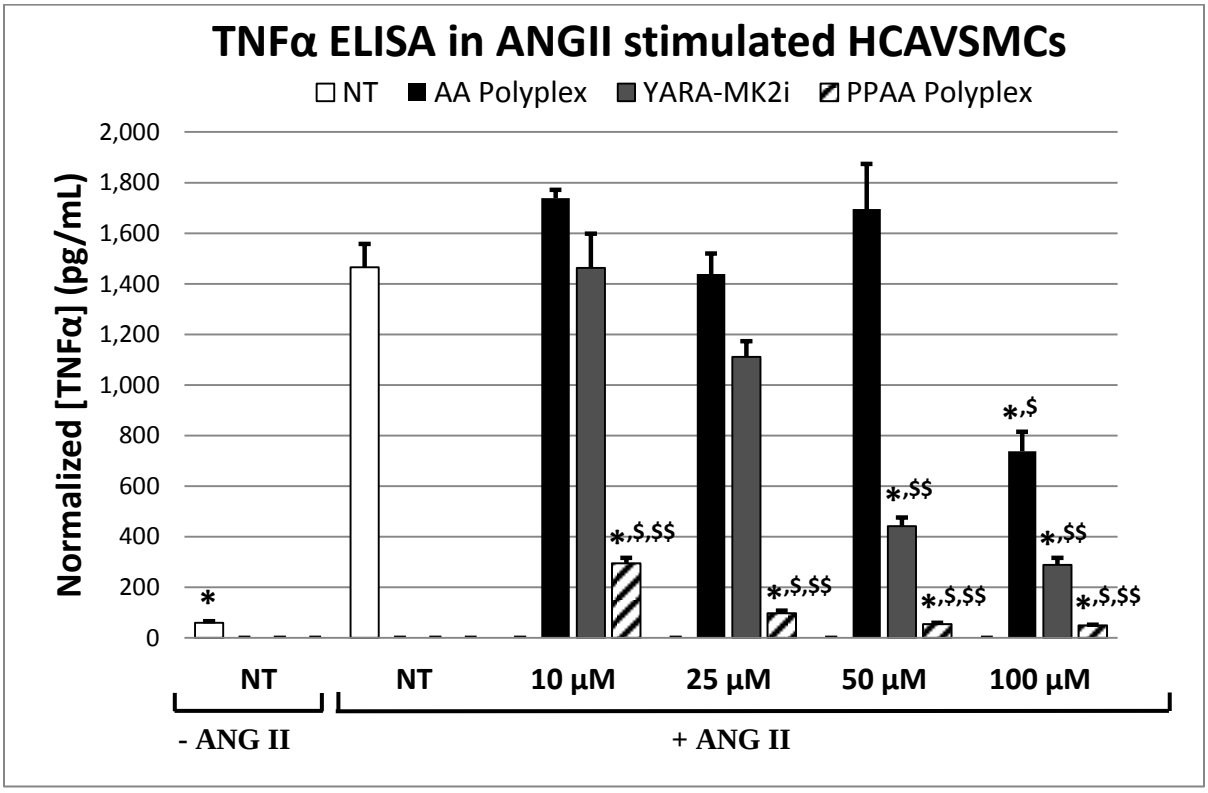

Figure 10 – Polyplex-mediated inhibition of TNFα production: TNFα production in HCAVSMCs stimulated with ANG II for 6 hours, treated for two hours with PPAA polyplexes, AA Polyplexes or the fusion MK2i peptide alone and cultured for 24 hours in fresh media. All data is normalized to cell number as determined by an LDH assay. Data for CPP polyplexes is not shown as all CPP polyplexes were found to upregulate TNFα production compared to the NT + TNFα group. NT = no treatment. *$p<0.05$ compared to NT + TNFα group, $^{\$}$ $p<0.05$ compared to MK2i at the same concentration, $^{\$\$}$ $p<0.05$ compared to AA polyplexes at the same concentration, $n = 4$.

Polyplex Uptake and Intracellular Trafficking

To study the effects of co-delivering a pH-responsive, endosomolytic polymer in conjunction with the YARA-MK2i peptide, a fluorescent carboxyfluorescein (FAM) label was conjugated to the YARA-MK2i peptide prior to formulating fluorescent polyplexes. Microscopic analysis revealed that initially the peptide alone is colocalized within endosomal compartments, however, polyplex treated cells demonstrate diffuse cytoplasmic fluorescence and decreased endo-lysosomal colocalization (see **fig. 11B**). Additionally, more intense fluorescence is noticeable in polyplex treated samples compared to peptide treated samples, which is indicative of increased uptake. At the 4 hours cells treated with polyplexes begin to show enlarged vesicles with diffuse green staining, indicative of active endosomal membrane destabilization and rupture. Punctate, colocalized staining remains in cells treated with the peptide alone out to 24 hours, whereas diffuse staining is apparent in polyplex treated samples out to 12 hours. These differences in endo-lysosomal colocalization can be quantified through the calculation of the Mander's coefficient, M1, defined as the ratio of the summed intensities of pixels in the green image for which the intensity in the red channel is above zero (the percentage of green FAM fluorophore that overlaps the red lysotracker fluorophore, where a value of 1 reflect 100% colocalization, see **fig. 11A**). The Mander's coefficient calculated for polylex treated cells were significantly less than cells treated with the peptide alone at all time points, with the peptide alone demonstrating near 100% colocalization at all time points. Interestingly, polyplex treated sampled evinced a time-dependent increase in colocalization at 10 and 22 hours of incubation, indicating that the cytoplasmic half-life of the peptide/fluorescence is lower than the endosomal half-life of the peptide/fluorescence, which could potentially be due to enzymatic degradation in the cytosol or introduction into a retrograde trafficking pathway.

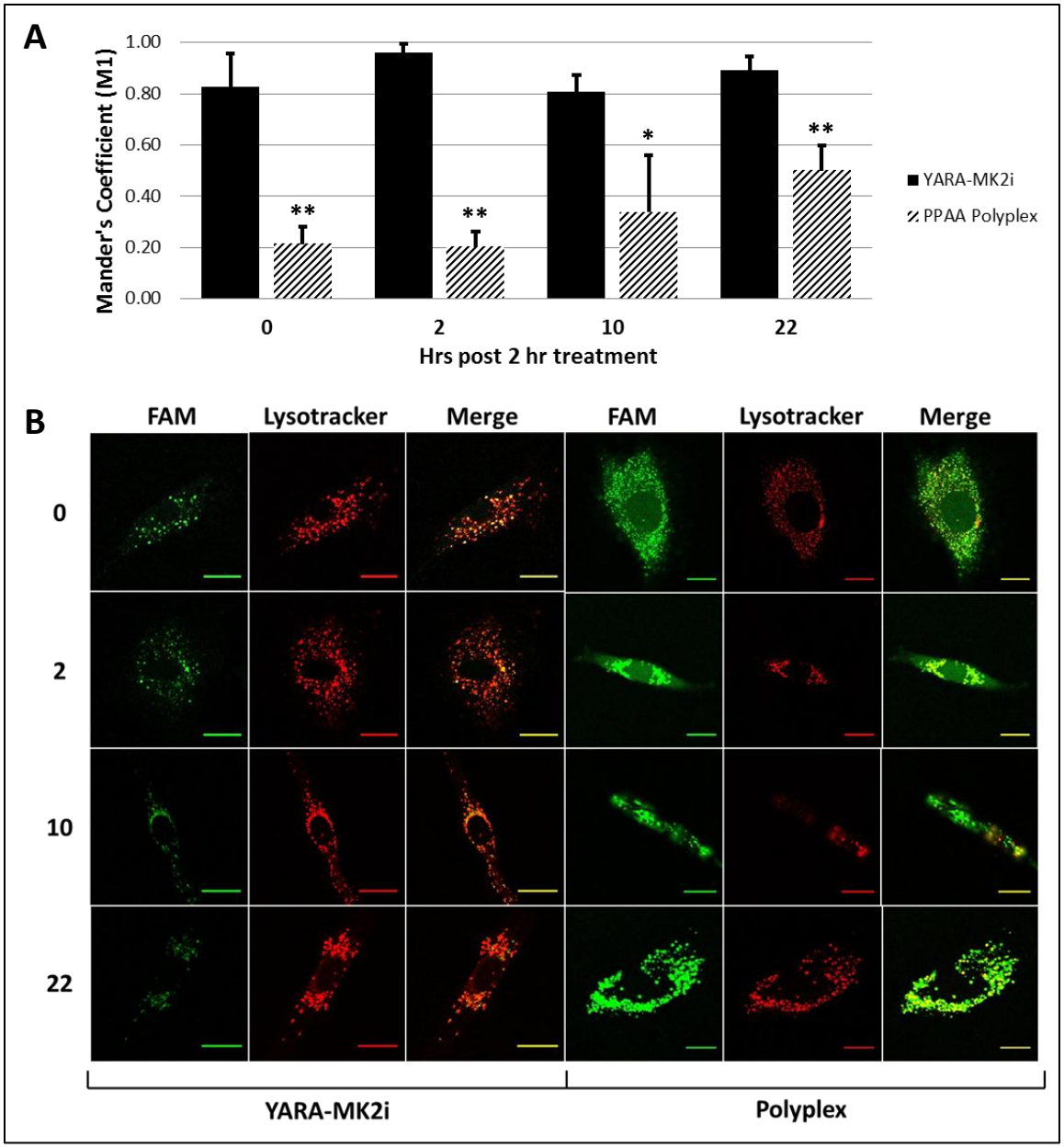

Figure 11 – Microscopic analysis of polyplex uptake: (A) Calculated Mander's coefficient, M1, defined as the ratio of the summed intensities of pixels in the green image for which the intensity in the red channel is above zero for HCAVSMCs treated for two hours with either fluorescently-labeled YARA-MK2i peptide or fluorescently-labeled polyplexes. YARA-MK2i dose = 25 μM for all samples. Values shown are the average n=3 separate images ± SEM. *p<0.05 compared to YARA-MK2i at the same time point, **p<0.01 compared to YARA-MK2i at the same time point **(B)** Representative fluorescence images used to quantify colocalization. The numbers on the left represent the amount of time the cells were incubated in fresh media following two hours of treatment, the gain for both the red and green channels was kept constant for all images obtained.

To quantify cellular uptake and assess differences in the intracellular half-life of polyplex vs. peptide treated cells, HCAVSMCs were treated with equivalent concentrations of fluorescently-labeled YARA-MK2i peptide or fluorescently-labeled polyplexes for 2 hours and then incubated for an additional 46 hours in fresh media. Flow cytometric analysis of cellular uptake and retention over time revealed significant differences ($p<0.05$) between polyplex and peptide treated cells (see **fig. 12**). Polyplex treated cells demonstrated a mean fluorescence 2 orders of magnitude higher than cells treated with the peptide alone or with AA polyplex vehicle controls despite being treated with the same concentration of fluorescently labeled peptide. The mean fluorescence intensity of peptide and AA polyplex treated samples decreased significantly over the 48 hours following the initial treatment, whereas PPAA polyplex treated samples still demonstrate robust fluorescence at 48 hours. These results indicate that both the peptide alone and AA polyplexes are exocytosed or degraded within the endo-lysosomal pathway. PPAA polyplex treated cells also show a decrease in fluorescence over time, but still demonstrate fluorescence at 48 hours that far exceeds the fluorescence seen at early time points in cells treated with the peptide alone or AA polyplexes. In order to more clearly represent the differences in retention of the peptide over time, an exponential model was used to quantify intracellular fluorescence half-lives for each treatment group as shown in equation 1:

$$Eqn\ 1: \qquad N(t) = N_o e^{-\lambda t}$$

Where N_o is the initial mean fluorescence intensity, and λ is the decay constant for the mean fluorescence intensity and can be used to calculate intracellular fluorescence half-life using equation 2:

$$Eqn\ 2: \qquad \tau_{1/2} = \frac{\ln(2)}{\lambda}$$

By calculating the intracellular fluorescence half-life the differences in cellular uptake and retention are more clearly demonstrated: polyplex treated cells have an initial mean fluorescence intensity of N_o =2,611 compared to N_o =28 and N_o =33 for YARA-MK2i and AA treated cells, representing difference of ~2 orders of magnitude in initial uptake. Furthermore, polyplexes yielded an intracellular half-life of $\tau_{1/2}$ = 117 hours compared to $\tau_{1/2}$ = 27 hours for both YARA-MK2i and AA Polyplex treated cells, signifying that polyplexes are not as prone to exocytosis and/or degradation in the endo-lysosomal pathway as the peptide alone.

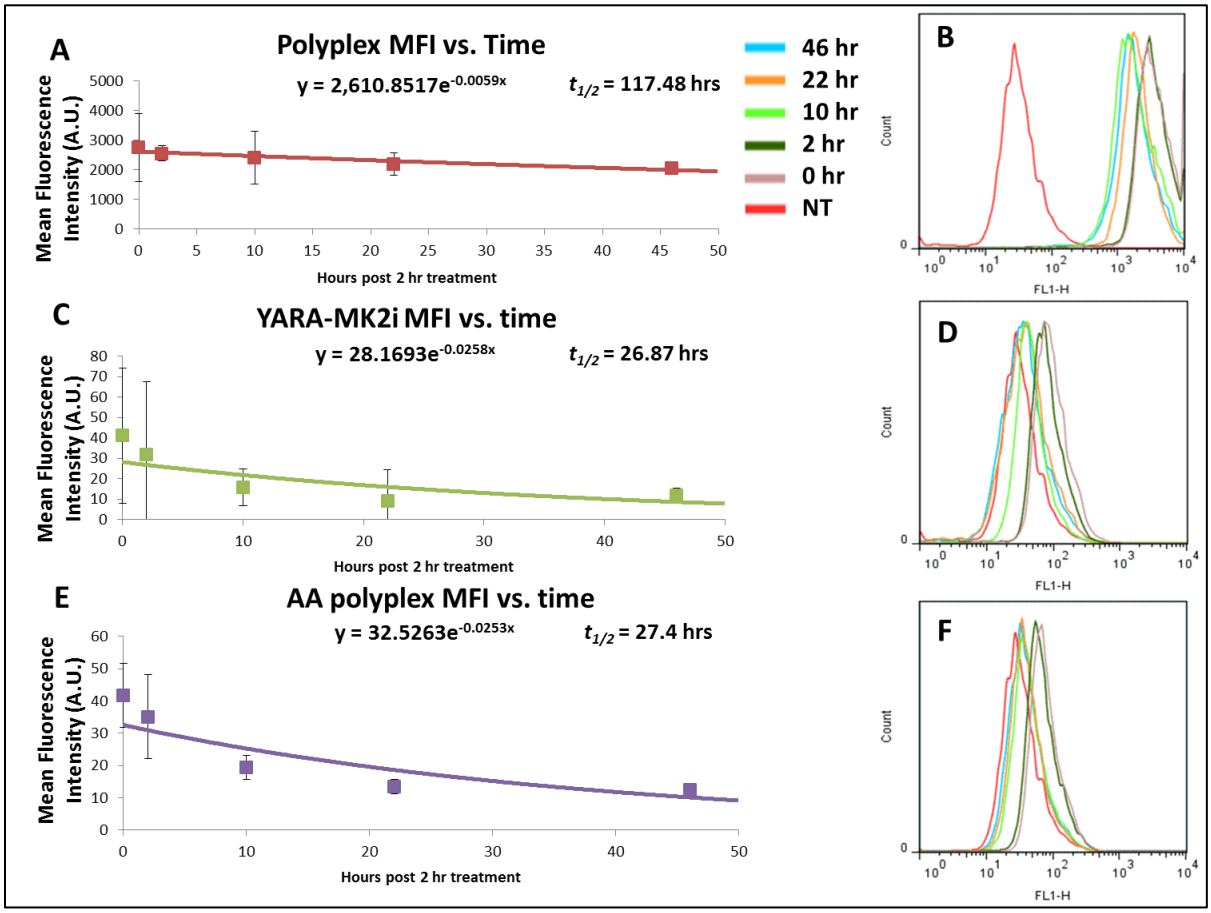

Figure 12 – Cellular uptake and intracellular half-life: Plots of mean fluorescence intensity over time and histograms of fluorescence intensity over time for PPAA polyplexes **(A,B)**, the YARA-MK2i peptide alone **(C,D)**, and AA polyplexes **(E,F)**. Exponential lines were fit to each data set in order to determine a fluorescence half-life for each treatment group. Mean Fluorescence Intensity values are reported as increase in MFI compared to untreated controls, n=3.

Discussion

Methods to enable the efficient intracellular delivery of peptide-based therapeutics are a potentially high-impact but relatively unmet need. This shortcoming is primarily due to multiple delivery barriers that exist in terms of delivering biomacromolecular therapeutics, each of which must be addressed to optimize bioactivity. In this work, a novel platform technology is presented that not only enhances the cellular uptake of a therapeutic peptide, but facilitates its escape from the endo-lysosomal pathway while containing an inherent mechanism to simultaneously release the peptide in the desired micro-environment.

The RAFT synthesized PPAA polymer serves as the key component of this nanotechnology platform for intracellular peptide delivery. The carboxylic acid groups present in the PPAA repeating unit has a pKa ~6.7, causing it to become protonated and membrane-disruptive at pH values encountered in the endo-lysosomal pathway as shown in **fig. 9a**. [49]. These carboxylic acid groups are deprotonated at pH values above the pKa of 6.7, rendering the polymer anionic at slightly basic pH values. This anionic behavior allows for electrostatic complexation with cationic peptides due to the presence of primary amines in specific amino acid side chains (pKa ~9-12 depending on the amino acid) and results in well-defined nano-polyplexes as shown in **figs 6-7**. Most peptide based therapeutics utilize a cell penetrating peptide to facilitate cellular uptake, and the majority of these cell penetrating peptides are cationic in nature (e.g. oligoarginines, oligolysines, TAT, penetratin, etc.) [23, 24, 50, 51]. As a result, this approach has the potential to serve as a platform technology for the intracellular delivery of a wide range of therapeutic peptides for a variety of applications. Furthermore, the electrostatic complexation of a cationic therapeutic and the anionic 'smart' polymer is reversible, allowing for 'de-complexation' and release of the peptide once the PPAA polymer becomes protonated due to electrostatic repulsion as shown in **fig. 9B-E**.

Shown in **fig. 1** is the signaling pathway targeted for validation of this approach to intracellular peptide delivery, as MAPKAP Kinase II is active in the cytoplasm and nucleus, and, as a result, an antagonist must be delivered into the cytosol in order to optimize bioactivity. A highly-specific, cell penetrant peptide antagonist of MK2 has been previously developed and proven to modulate VSMC phenotype and prevent intimal hyperplasia in human saphenous vein [52], but peptides utilizing this CPP sequence have been shown to become trapped in the endo-lysosomal pathway [19]. However, through the incorporation of this cationic peptide into an endosomolytic nano-polyplex that contains an endosomolytic 'smart' polymer this endosomal entrapment can be overcome as seen in the pH dependent membrane disruption seen in **fig 8** and the diffuse staining pattern present in polyplex treated cells in **fig. 11**. Enhanced cytoplasmic delivery of this peptide should concomitantly increase its bioactivity and effectively reduce the half maximal inhibitory concentration, or IC50, of the therapeutic being delivered [53]. **Figs 9-10** verify this endosomolytic

enhancement in bioactivity through well-established *in vitro* assays to assess VSMC phenotype [47, 48].

It is well-established that peptides, not to mention other biomacromolecules like siRNA and DNA, suffer from poor cellular uptake when administered alone. As a result, cell penetrating peptides, fusogenic peptides, or targeting ligands are utilized to facilitate/enhance cellular uptake [51]. Despite the fact that the fusion peptide utilized in this work contains a cell-penetrating peptide sequence, formulation into a nano-polyplex results in a much more significant increase in uptake as shown in **figs. 11-12**. This finding is interesting in that providing a net-positive charge typically facilitates optimal cellular uptake [54] [55], yet the polyplexes developed demonstrated a net negative charge as shown by ζ-potential measurements in **fig. 6**. Fluorescence measurements were also performed on the supernatant of treated cells to look at fluorescently labeled peptide or polyplexes left in solution, and a clear difference was noted that correlated with the differences in uptake seen through microscopy and flow cytometric analysis (data not shown). Furthermore, the buffering capacity of the polyplexes may provide a means of cargo protection, since more acidic environments are typically more prone to degrade biologic drugs. Once internalized, the duration of efficacy of the delivered peptide is dependent on rates of exocytosis, endo-lysosomal degradation, and cytoplasmic degradation. It is well established that free peptides in the cytosol are short-lived and rapidly broken down by intracellular proteolytic complexes (e.g. the ATP-dependent 26 S proteasome) [56]; our results suggest that complexation with the PPAA polymer may stabilize the YARA-MK2i peptide and help sustain its bioactivity. Previous *in vivo* time course studies have shown that utilizing the YARA-MK2i peptide will delay the onset of intimal hyperplasia in vein grafts, but only appears to delay the onset of intimal thickening by ~ 1 week [57]. However, as shown in **fig. 12**, the cellular half-life of the peptide is significantly prolonged through delivery in the form of an endosomolytic polyplex, and thus, may increase the duration of efficacy of the peptide when used in bypass grafting applications.

It is hypothesized that when the nanotechnology presented here is translated *in vivo*, that the enhanced uptake and intracellular half-life demonstrated *in vitro* will results in optimized protein delivery that minimizes the dose of peptide required and will prolong the duration of efficacy of the treatment. However, further studies will be necessary to better understand the underlying mechanism

of enhanced uptake and to corroborate the increase in intracellular half-life seen in preliminary results. Furthermore, *ex vivo* and *in vivo* studies will be necessary to evaluate the clinical translatability of this approach as a platform technology for intracellular peptide delivery.

Conclusion

Well defined, pH-responsive, endosomolytic nano-polyplexes were successfully synthesized and utilized to enhance the intracellular delivery and endosomal escape of a therapeutic MK2 inhibitor peptide. The synthesized nano-polyplexes demonstrated a significantly enhanced ability to facilitate cellular uptake of a therapeutic peptide and conjointly enhance its intracellular half-life. Furthermore, the increase in cell uptake and cellular half-life correlated well with *in vitro* enhancement of peptide bioactivity. Due to the modular nature of this approach, these nano-polyplexes can be adapted to a number of cationic biomacromolecular drugs, serving as a platform technology that not only has potential as a high-impact clinical tool but also provides a logical approach to studying the effect of intracellular-acting therapeutics. Finally, the described technology shows therapeutic potential as a preventative treatment in vascular bypass grafting applications, and may also show promise as a treatment for a myriad of human diseases.

CHAPTER III

ONGOING AND FUTURE WORK

Elucidating Method of Polyplex Uptake and Intracellular Trafficking

Based on the preliminary cellular uptake studies presented in Chapter II, polyplexes demonstrated a profound increase in cellular uptake that was not expected due to a slightly negative ζ-potential. However, this drastic discrepancy may be in part due to the pH-sensitivity of the fluorophore utilized. In order to provide a more accurate description of differences in cellular uptake and intracellular trafficking, an alternative fluorophore label can be used that does not exhibit pH-sensitive fluorescence (i.e. Alexa488, which shows stable fluorescence at pH values ranging from 4-10). Fluorescence microscopy and flow cytometry studies will be repeated with an alternative fluorophore in order to corroborate the enhanced cellular uptake noted. Furthermore, the ratio in fluorescence intensity between pH-sensitive and a pH-insensitive fluorophores can be used as an indicator of the subcellular pH distribution encountered by the internalized therapeutics [58]. In order to more fully understand the underlying uptake mechanism that results in such a drastic differences in cellular uptake, a variety of cellular uptake assays that utilize inhibitors of specific cellular processes can be used to elucidate the mechanism of polyplex uptake [59]. Furthermore, plasmids containing a promotor sequence specific to various intracellular trafficking pathways can be used to transfect and monitor cells that are actively trafficking peptides delivered in polyplex form [19]. These studies will be key to understanding the mechanism of increased uptake and modulation of intracellular trafficking facilitated by these pH-responsive nano-polyplexes.

Quantifying Duration of Efficacy

Initial results indicate that the use of endosomolytic polyplexes to deliver a therapeutic peptide not only enhances uptake but increase the intracellular half-life of the therapeutic. This increase in intracellular half-life may potentially result in an increase in the duration of efficacy of the treatment. The duration of efficacy of these treatments can be more fully assayed through time

course studies that extend beyond the time points used in this work. Microscopic analysis of uptake and flow cytometric studies can be utilized to provide a more complete picture of peptide uptake, exocytosis, and degradation. Furthermore, pulse-chase *in vitro* assays, such as the inflammatory cytokine analyses performed in this work, can be adapted to provide a more thorough understanding of the temporal dynamics of peptide bioactivity.

Ex Vivo and *In Vivo* Testing

Vascular and molecular biologist have made tremendous advances in understanding and treating vascular pathologies like coronary heart disease. This body of work presents a novel therapeutic approach that can potentially be translated into clinical use for the treatment of vessels used in bypass grafting procedures. To evaluate the potential of this technology *ex vivo* assays can be utilized to assess polyplex mediated vasorelaxation of human saphenous vein explants. Furthermore, human saphenous vein explants can be utilized in an organ culture model to assess the potential of the developed polyplexes to inhibit intimal hyperplasia in human tissue. Upon validation of therapeutic efficacy, a more robust rabbit carotid interposition *in vivo* model will be used to verify treatment efficacy in a clinically relevant vascular bypass grafting application

Adaptation to Other Therapeutics and Applications

This drug delivery approach has demonstrated the potential to be utilized as a platform technology to facilitate intracellular peptide delivery, but the applicability of this approach to other peptide-based drugs and other applications has yet to be validated. The YARA-MK2i peptide described may be beneficial for a number of disease states including but not limited to asthma [60], inflammatory disease [60], Alzheimer's disease [61, 62], cancer [63], and rheumatoid arthritis [64]. Thus, a library of endosomolytic nano-polyplexes containing a variety of different peptide-based therapeutics can be synthesized and characterized in order to determine the utility of this approach as a platform technology. In addition, this approach enables the topical or local treatment of target tissues, but does not allow for intravenous administration of a peptide-based drug. In order to facilitate hemocompatibility and prolong circulatory half-life, various other polyplex/nano-carrier

design schemes can be tested that utilize the same endosomolytic ‘smart’ polymer technology. For instance, a diblock copolymer containing the pH-responsive poly(propylacrylic acid) ‘smart’ polymer and a biocompatible, hydrophilic block [e.g. poly(ethylene glycol) (PEG) or poly(hydroxypropyl) methacrylamide (HPMA)] could potentially be utilized to formulate micellar nanoparticles that contain electrostatically-complexed biomacromolecular therapeutics in the pH-responsive core of the construct.

APPENDIX

Appendix A: PPAA GPC analysis

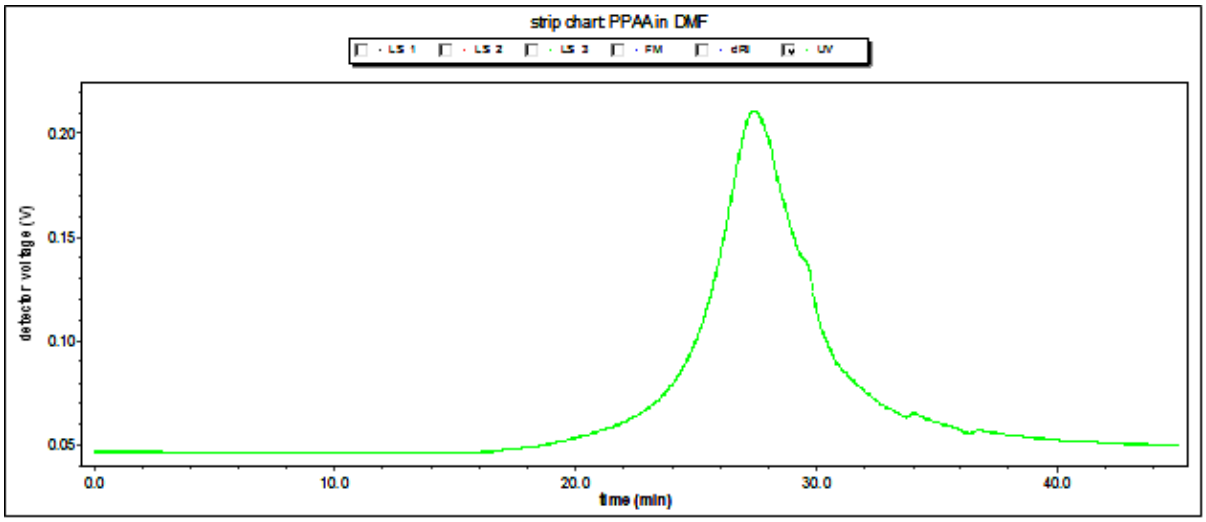

Supplementary Figure 1: GPC chromatogram of poly(propylacrylic acid) (PPAA) homopolymer in DMF. The trace shows UV absorbance at the characteristic absorption peak of the trithiocarbonate moiety (310 nm) present in the 4-cyano-4-(ethylsulfanylthiocarbonyl) sulfanylvpentanoic acid (ECT) chain transfer agent utilized in the polymerization. MW = 22,010, PDI =1.471, dη/dC = 0.087 (mL/g).

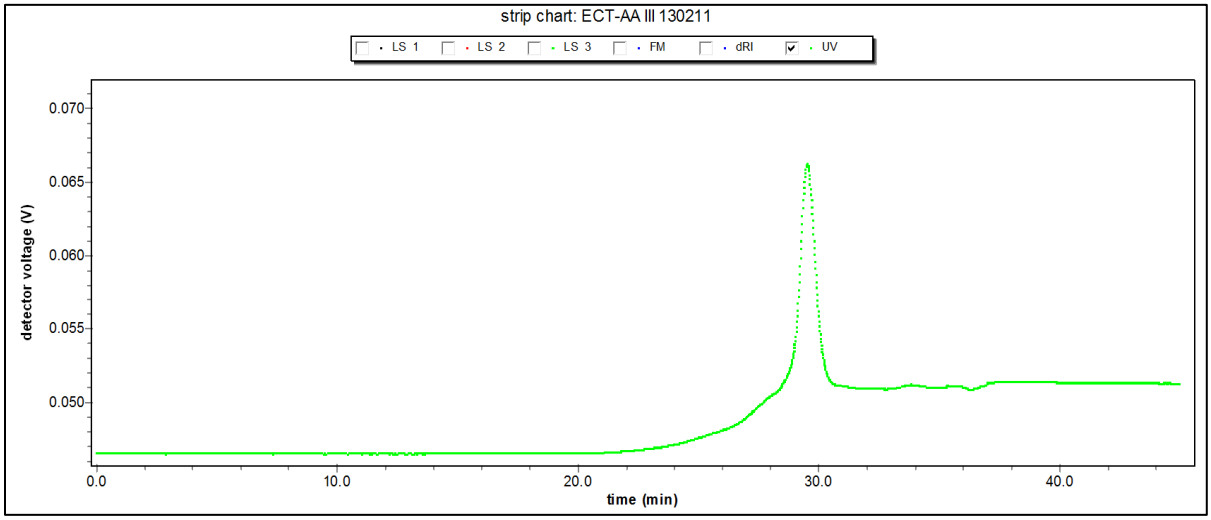

Supplementary Figure 2: GPC chromatogram of poly(acrylic acid) (AA) homopolymer in DMF. The trace shows UV absorbance at the characteristic absorption peak of the trithiocarbonate moiety (310 nm) present in the 4-cyano-4-(ethylsulfanylthiocarbonyl) sulfanylvpentanoic acid (ECT) chain transfer agent utilized in the polymerization. MW = 10,830, PDI =1.273, dη/dC = 0.09 (mL/g).

Appendix B: ^{1}H NMR Spectra

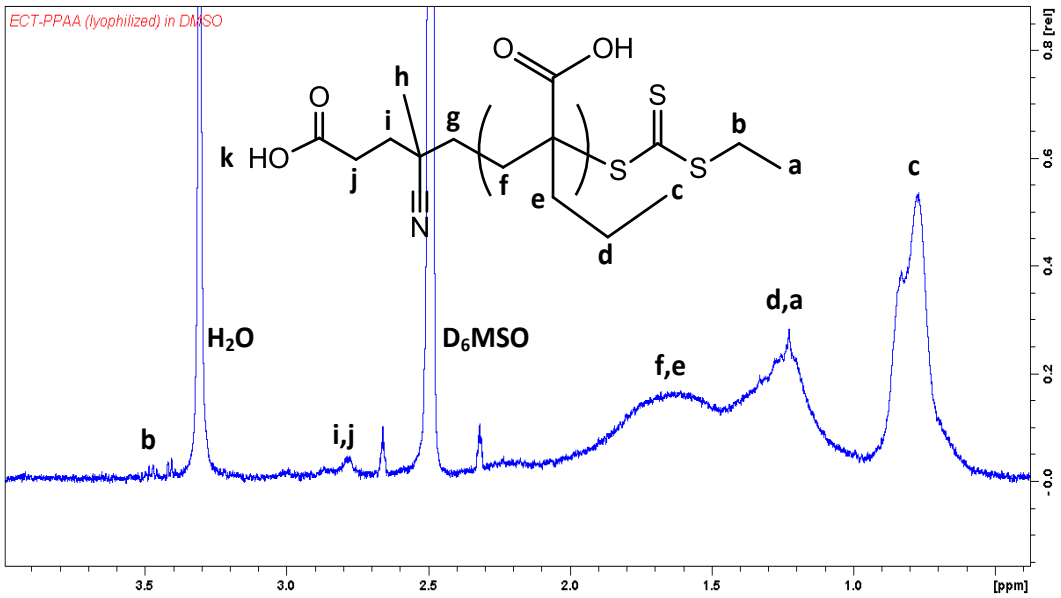

Supplementary Figure 3: ^{1}H NMR spectrum of poly(propylacrylic acid) (PPAA) homopolymer in D_6MSO. Molecular weight was determined by comparing the area of peaks associated with the chain transfer agent (i.e. peak b) to peaks associated propylacrylic acid (i.e. peak c): Degree of polymerization = 190, MW = 21,950 g/mol).

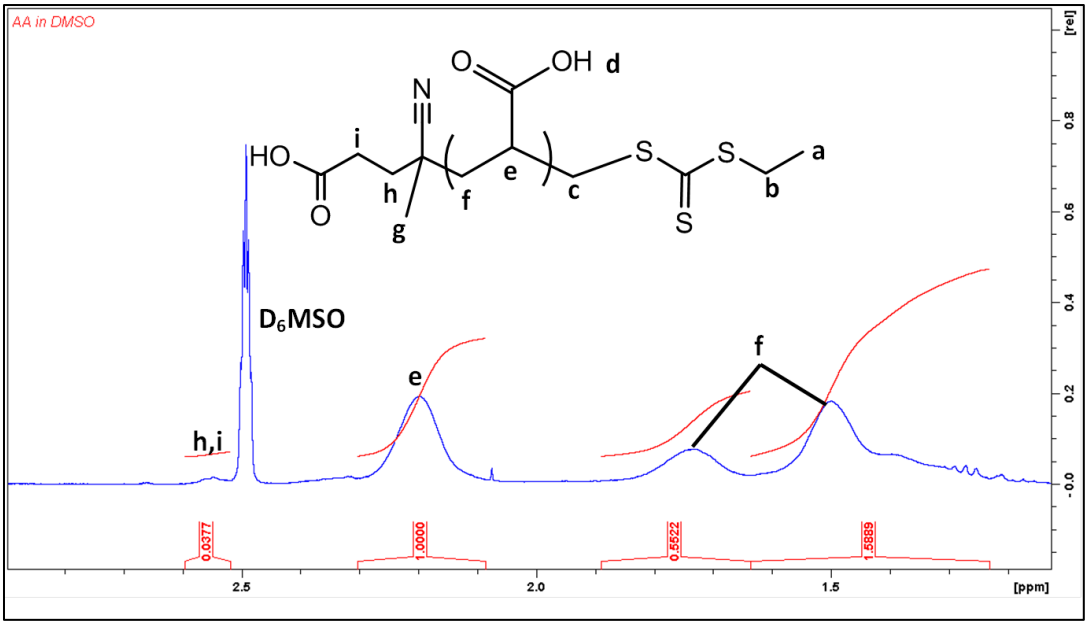

Supplementary Figure 4: ^{1}H NMR spectrum of poly(acrylic acid) (AA) homopolymer in D_6MSO. Molecular weight was determined by comparing the area of peaks associated with the chain transfer agent (i.e. peaks h,i) to peaks associated with acrylic acid (i.e. peak e): Degree of polymerization = 106, MW = 7,640 g/mol).

Appendix C: Polyplex Cytotoxicity

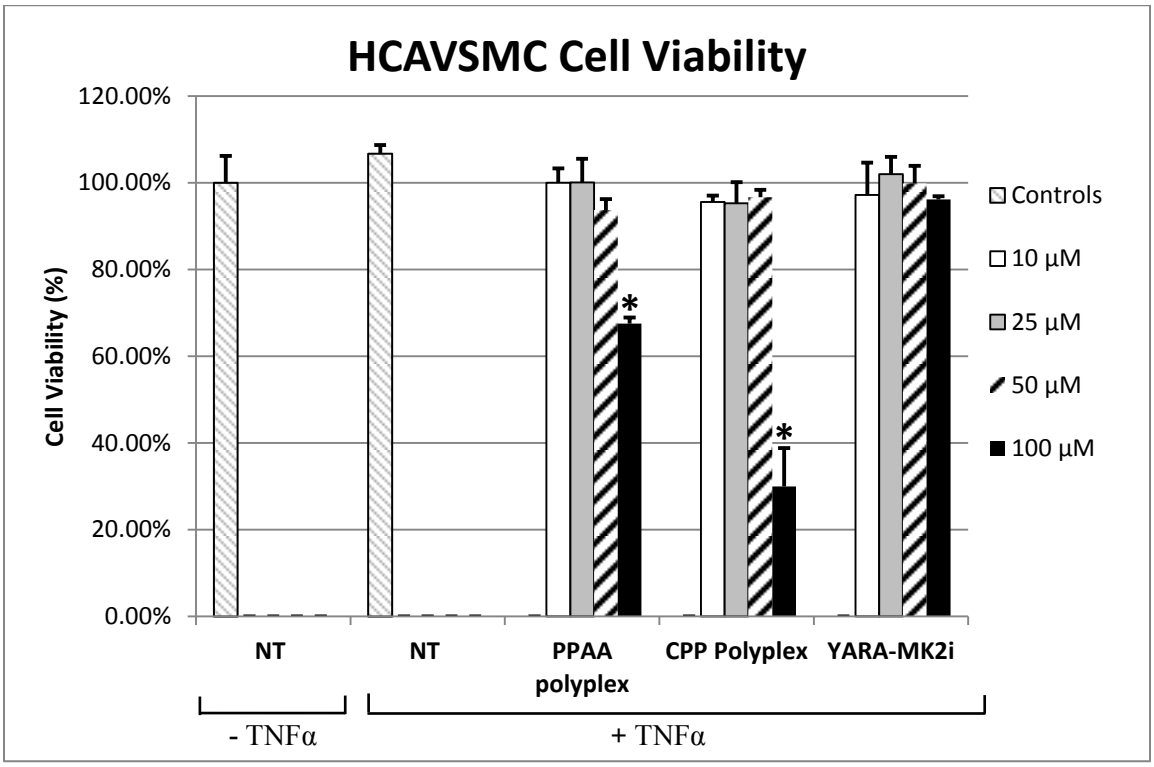

Supplementary Figure 5: Cell viability in HCAVSMCs stimulated with TNFα for 6 hours, treated for two hours with polyplexes (containing the full fusion sequence or the CPP alone) or the fusion MK2i peptide and cultured for 24 hours in fresh media. NT = no treatment. *p<0.01 compared to NT + TNFα group, n = 4.

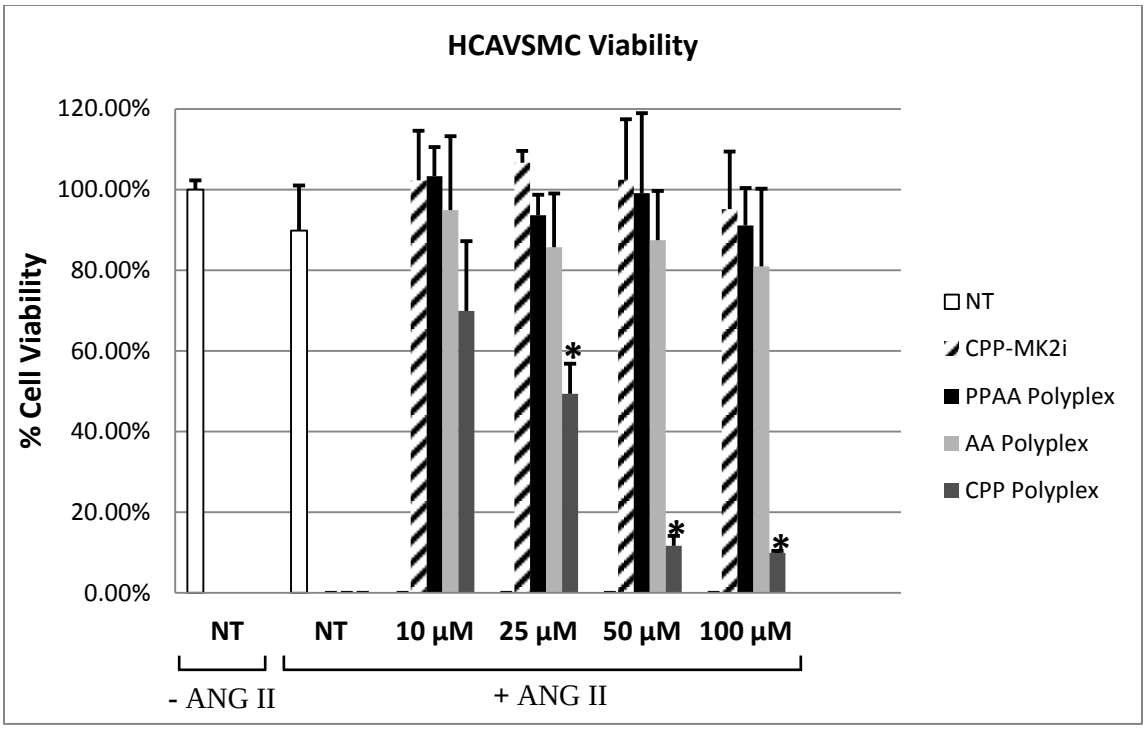

Supplementary Figure 6: Cell viability in HCAVSMCs stimulated with 10 µM ANG II for 6 hours, treated for two hours with polyplexes (containing the full fusion sequence with PPAA, the full fusion sequence with AA, or the CPP alone) or the fusion MK2i peptide and cultured for 24 hours in fresh media. NT = no treatment. *$p<0.01$ compared to NT – ANG II group, n = 4.

REFERENCES

1. Go, A.S., et al., *Heart disease and stroke statistics--2013 update: a report from the American Heart Association.* Circulation, 2013. **127**(1): p. e6-e245.
2. Alexander, J.H., et al., *Efficacy and safety of edifoligide, an E2F transcription factor decoy, for prevention of vein graft failure following coronary artery bypass graft surgery: PREVENT IV: a randomized controlled trial.* JAMA, 2005. **294**(19): p. 2446-54.
3. Raingeaud, J., et al., *Pro-inflammatory cytokines and environmental stress cause p38 mitogen-activated protein kinase activation by dual phosphorylation on tyrosine and threonine.* J Biol Chem, 1995. **270**(13): p. 7420-6.
4. Lopes, L.B., et al., *A novel cell permeant peptide inhibitor of MAPKAP kinase II inhibits intimal hyperplasia in a human saphenous vein organ culture model.* J Vasc Surg, 2010. **52**(6): p. 1596-607.
5. Chen, H.F., L.D. Xie, and C.S. Xu, *Role of heat shock protein 27 phosphorylation in migration of vascular smooth muscle cells.* Mol Cell Biochem, 2009. **327**(1-2): p. 1-6.
6. Zarubin, T. and J.H. Han, *Activation and signaling of the p38 MAP kinase pathway.* Cell Research, 2005. **15**(1): p. 11-18.
7. Ward, B., et al., *Design of a bioactive cell-penetrating peptide: when a transduction domain does more than transduce.* Journal of Peptide Science, 2009. **15**(10): p. 668-674.
8. Hayess, K. and R. Benndorf, *Effect of protein kinase inhibitors on activity of mammalian small heat-shock protein (HSP25) kinase.* Biochem Pharmacol, 1997. **53**(9): p. 1239-47.
9. Duvall, C.L., et al., *Intracellular delivery of a proapoptotic peptide via conjugation to a RAFT synthesized endosomolytic polymer.* Mol Pharm, 2010. **7**(2): p. 468-76.

10. Wilson, T.R., P.G. Johnston, and D.B. Longley, *Anti-apoptotic mechanisms of drug resistance in cancer.* Curr Cancer Drug Targets, 2009. **9**(3): p. 307-19.

11. Alexander, J.H., et al., *Efficacy and safety of edifoligide, an E2F transcription factor decoy, for prevention of vein graft failure following coronary artery bypass graft surgery - PREVENT IV: A randomized controlled trial.* Jama-Journal of the American Medical Association, 2005. **294**(19): p. 2446-2454.

12. Craik, D.J., et al., *The Future of Peptide-based Drugs.* Chemical Biology & Drug Design, 2013. **81**(1): p. 136-147.

13. Ewing, M.M., et al., *Annexin A5 Therapy Attenuates Vascular Inflammation and Remodeling and Improves Endothelial Function in Mice.* Arteriosclerosis Thrombosis and Vascular Biology, 2011. **31**(1): p. 95-+.

14. Gizard, F. and D. Bruemmer, *Transcriptional Control of Vascular Smooth Muscle Cell Proliferation by Peroxisome Proliferator-Activated Receptor-gamma: Therapeutic Implications for Cardiovascular Diseases.* Ppar Research, 2008.

15. Ni, J., A. Waldman, and L.M. Khachigian, *c-Jun Regulates Shear- and Injury-inducible Egr-1 Expression, Vein Graft Stenosis after Autologous End-to-Side Transplantation in Rabbits, and Intimal Hyperplasia in Human Saphenous Veins.* Journal of Biological Chemistry, 2010. **285**(6): p. 4038-4048.

16. Hata, J.A., et al., *Modulation of phosphatidylinositol 3-kinase signaling reduces intimal hyperplasia in aortocoronary saphenous vein grafts.* Journal of Thoracic and Cardiovascular Surgery, 2005. **129**(6): p. 1405-1413.

17. Al-Taei, S., et al., *Intracellular traffic and fate of protein transduction domains HIV-1 TAT peptide and octaarginine. Implications for their utilization as drug delivery vectors.* Bioconjug Chem, 2006. **17**(1): p. 90-100.

18. Belting, M., S. Sandgren, and A. Wittrup, *Nuclear delivery of macromolecules: barriers and carriers.* Adv Drug Deliv Rev, 2005. **57**(4): p. 505-27.

19. Flynn, C.R., et al., *Internalization and intracellular trafficking of a PTD-conjugated anti-fibrotic peptide, AZX100, in human dermal keloid fibroblasts.* J Pharm Sci, 2010. **99**(7): p. 3100-21.

20. Chorev, M., et al., *Partially Modified Retro-Inverso-Peptides - Novel Modification of Biologically-Active Peptides.* Federation Proceedings, 1979. **38**(3): p. 363-363.

21. Taylor, J.W., *The synthesis and study of side-chain lactam-bridged peptides.* Biopolymers, 2002. **66**(1): p. 49-75.

22. Kritzer, J.A., *STAPLED PEPTIDES Magic bullets in nature's arsenal.* Nature Chemical Biology, 2010. **6**(8): p. 566-567.

23. Cahill, K., *Cell-penetrating peptides, electroporation and drug delivery.* Iet Systems Biology, 2010. **4**(6): p. 367-378.

24. De Coupade, C., et al., *Novel human-derived cell-penetrating peptides for specific subcellular delivery of therapeutic biomolecules.* Biochemical Journal, 2005. **390**: p. 407-418.

25. Efremov, R.G., et al., *Factors important for fusogenic activity of peptides: molecular modeling study of analogs of fusion peptide of influenza virus hemagglutinin.* Febs Letters, 1999. **462**(1-2): p. 205-210.

26. Ayame, H., N. Morimoto, and K. Akiyoshi, *Self-assembled cationic nanogels for intracellular protein delivery.* Bioconjugate Chemistry, 2008. **19**(4): p. 882-890.

27. Ko, Y.T., C. Falcao, and V.P. Torchilin, *Cationic Liposomes Loaded with Proapoptotic Peptide D-(KLAKLAK)(2) and Bcl-2 Antisense Oligodeoxynucleotide G3139 for Enhanced Anticancer Therapy.* Molecular Pharmaceutics, 2009. **6**(3): p. 971-977.

28. Yamada, Y., et al., *Mitochondrial drug delivery and mitochondrial disease therapy - An approach to liposome-based delivery targeted to mitochondria.* Mitochondrion, 2007. **7**(1-2): p. 63-71.

29. Li, H., et al., *Delivery of intracellular-acting biologics in pro-apoptotic therapies.* Curr Pharm Des, 2011. **17**(3): p. 293-319.

30. Zhao, P.Q., et al., *Paclitaxel-Loaded, Folic-Acid-Targeted and TAT-Peptide-Conjugated Polymeric Liposomes: In Vitro and In Vivo Evaluation.* Pharmaceutical Research, 2010. **27**(9): p. 1914-1926.

31. El-Sayed, A., et al., *Octaarginine- and octalysine-modified nanoparticles have different modes of endosomal escape.* Journal of Biological Chemistry, 2008. **283**(34): p. 23450-23461.

32. Kuai, R., et al., *Efficient Delivery of Payload into Tumor Cells in a Controlled Manner by TAT and Thiolytic Cleavable PEG Co-Modified Liposomes.* Molecular Pharmaceutics, 2010. **7**(5): p. 1816-1826.

33. Lackey, C.A., et al., *A biomimetic pH-responsive polymer directs endosomal release and intracellular delivery of an endocytosed antibody complex.* Bioconjugate Chemistry, 2002. **13**(5): p. 996-1001.

34. Henry, S.M., et al., *pH-responsive poly(styrene-alt-maleic anhydride) alkylamide copolymers for intracellular drug delivery.* Biomacromolecules, 2006. **7**(8): p. 2407-2414.

35. Murthy, N., et al., *Design and synthesis of pH-responsive polymeric carriers that target uptake and enhance the intracellular delivery of oligonucleotides.* Journal of Controlled Release, 2003. **89**(3): p. 365-74.

36. Jamieson, A.G., et al., *Peptide Scanning for Studying Structure-Activity Relationships in Drug Discovery.* Chemical Biology & Drug Design, 2013. **81**(1): p. 148-165.

37. Murthy, N., et al., *Bioinspired pH-responsive polymers for the intracellular delivery of biomolecular drugs.* Bioconjug Chem, 2003. **14**(2): p. 412-9.

38. Moad, G., et al., *Living free radical polymerization with reversible addition-fragmentation chain transfer (the life of RAFT).* Polymer International, 2000. **49**(9): p. 993-1001.

39. Boyer, C., et al., *Bioapplications of RAFT Polymerization.* Chemical Reviews, 2009. **109**(11): p. 5402-5436.

40. Jain, N.K., V. Mishra, and N.K. Mehra, *Targeted drug delivery to macrophages.* Expert Opinion on Drug Delivery, 2013. **10**(3): p. 353-367.

41. Crownover, E.F., A.J. Convertine, and P.S. Stayton, *pH-responsive polymer-antigen vaccine bioconjugates.* Polymer Chemistry, 2011. **2**(7): p. 1499-1504.

42. Convertine, A.J., et al., *Development of a novel endosomolytic diblock copolymer for siRNA delivery.* Journal of Controlled Release, 2009. **133**(3): p. 221-229.

43. Moad, G., et al., *Advances in RAFT polymerization: the synthesis of polymers with defined end-groups.* Polymer, 2005. **46**(19): p. 8458-8468.

44. Ferrito M, T.D., *Poly(2-ethylacrylic acid).* Macromol Synth, 1992(11): p. 59-62.

45. Evans, B.C., Nelson, C. E., Yu, S. S., Beavers, K. R., Kim, A. J., Li, H., et al., *Ex Vivo Red Blood Cell Hemolysis Assay for the Evaluation of pH-responsive Endosomolytic Agents for Cytosolic Delivery of Biomacromolecular Drugs.* J. Vis. Exp., 2013. **(73)**.

46. Bolte, S. and F.P. Cordelieres, *A guided tour into subcellular colocalization analysis in light microscopy.* Journal of Microscopy-Oxford, 2006. **224**: p. 213-232.

47. Taniyama, Y., et al., *Role of p38 MAPK and MAPKAPK-2 in angiotensin II-induced Akt activation in vascular smooth muscle cells.* American Journal of Physiology-Cell Physiology, 2004. **287**(2): p. C494-C499.

48. Ronkina, N., et al., *The mitogen-activated protein kinase (MAPK)-activated protein kinases MK2 and MK3 cooperate in stimulation of tumor necrosis factor biosynthesis and stabilization of p38 MAPK.* Molecular and Cellular Biology, 2007. **27**(1): p. 170-181.

49. Kyriakides, T.R., et al., *pH-sensitive polymers that enhance intracellular drug delivery in vivo.* Journal of Controlled Release, 2002. **78**(1-3): p. 295-303.

50. Bitler, B.G. and J.A. Schroeder, *Anti-cancer therapies that utilize cell penetrating peptides.* Recent Pat Anticancer Drug Discov, 2010. **5**(2): p. 99-108.

51. Heitz, F., M.C. Morris, and G. Divita, *Twenty years of cell-penetrating peptides: from molecular mechanisms to therapeutics.* British Journal of Pharmacology, 2009. **157**(2): p. 195-206.

52. Lopes, L.B., et al., *A novel cell permeant peptide inhibitor of MAPKAP kinase II inhibits intimal hyperplasia in a human saphenous vein organ culture model.* Journal of Vascular Surgery, 2010. **52**(6): p. 1596-1607.

53. Duncan, R. and S.C. Richardson, *Endocytosis and intracellular trafficking as gateways for nanomedicine delivery: opportunities and challenges.* Mol Pharm, 2012. **9**(9): p. 2380-402.

54. van der Aa, M.A.E.M., et al., *Cellular uptake of cationic polymer-DNA complexes via caveolae plays a pivotal role in gene transfection in COS-7 cells.* Pharmaceutical Research, 2007. **24**(8): p. 1590-1598.

55. Cho, Y.W., J.D. Kim, and K. Park, *Pollycation gene delivery systems: escape from endosomes to cytosol.* Journal of Pharmacy and Pharmacology, 2003. **55**(6): p. 721-734.

56. Saric, T., C.I. Graef, and A.L. Goldberg, *Pathway for degradation of peptides generated by proteasomes - A key role for thimet oligopeptidase and other metallopeptidases.* Journal of Biological Chemistry, 2004. **279**(45): p. 46723-46732.

57. Muto, A., et al., *Inhibition of Mitogen Activated Protein Kinase Activated Protein Kinase II with MMI-0100 reduces intimal hyperplasia ex vivo and in vivo.* Vascular Pharmacology, 2012. **56**(1-2): p. 47-55.

58. Berguig, G.Y., et al., *Intracellular Delivery and Trafficking Dynamics of a Lymphoma-Targeting Antibody-Polymer Conjugate.* Molecular Pharmaceutics, 2012. **9**(12): p. 3506-3514.

59. Duchardt, F., et al., *A comprehensive model for the cellular uptake of cationic cell-penetrating peptides.* Traffic, 2007. **8**(7): p. 848-866.

60. Gorska, M.M., et al., *MK2 controls the level of negative feedback in the NF-kappa B pathway and is essential for vascular permeability and airway inflammation.* Journal of Experimental Medicine, 2007. **204**(7): p. 1637-1652.

61. Thomas, T., et al., *MAP-kinase-activated protein kinase 2 expression and activity is induced after neuronal depolarization.* European Journal of Neuroscience, 2008. **28**(4): p. 642-654.

62. Culbert, A.A., et al., *MAPK-activated protein kinase 2 deficiency in microglia inhibits pro-inflammatory mediator release and resultant neurotoxicity - Relevance to neuroinflammation in a transgenic mouse model of Alzheimer disease.* Journal of Biological Chemistry, 2006. **281**(33): p. 23658-23667.

63. Reinhardt, H.C., et al., *p53-deficient cells rely on ATM- and ATR-mediated checkpoint signaling through the p38MAPK/MK2 pathway for survival after DNA damage.* Cancer Cell, 2007. **11**(2): p. 175-189.

64. Gaestel, M., et al., *Protein kinases as small molecule inhibitor targets in inflammation.* Current Medicinal Chemistry, 2007. **14**(21): p. 2214-2234.